Neutrons

Photons

The Complementarity of Real Space and Reciprocal Space

Lecture at Neutron and X-Ray School

J. Murray Gibson

June 12, 2009

Electrons?

Outline

- Hour 1 – theory
  - Imaging/diffraction and Fourier optics
  - electrons, x-rays and neutrons….
- Hour 2 – examples
  - Picking the right tool for the problem

emphasize electron and x-ray microscopy as complementary tools

Why real-space?

- Yawn
  - I thought we were there already….
- Magnification
  - direct imaging of atoms..
- Diffraction Contrast
  - fourier optics

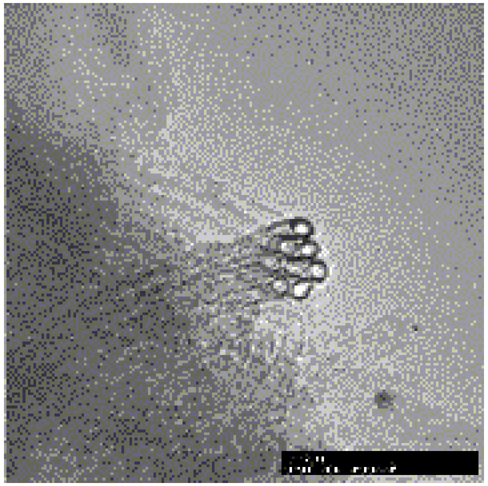

Smalley, Rice University

Microscopy with diffracting radiation

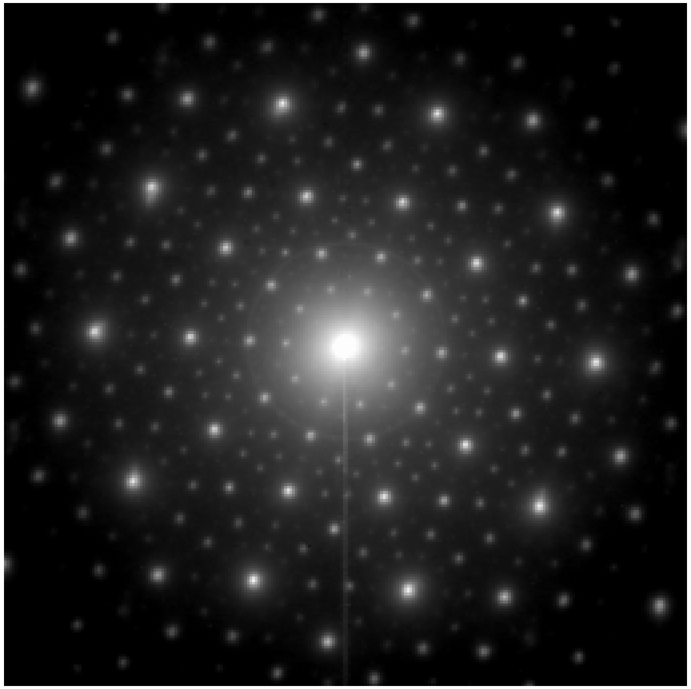

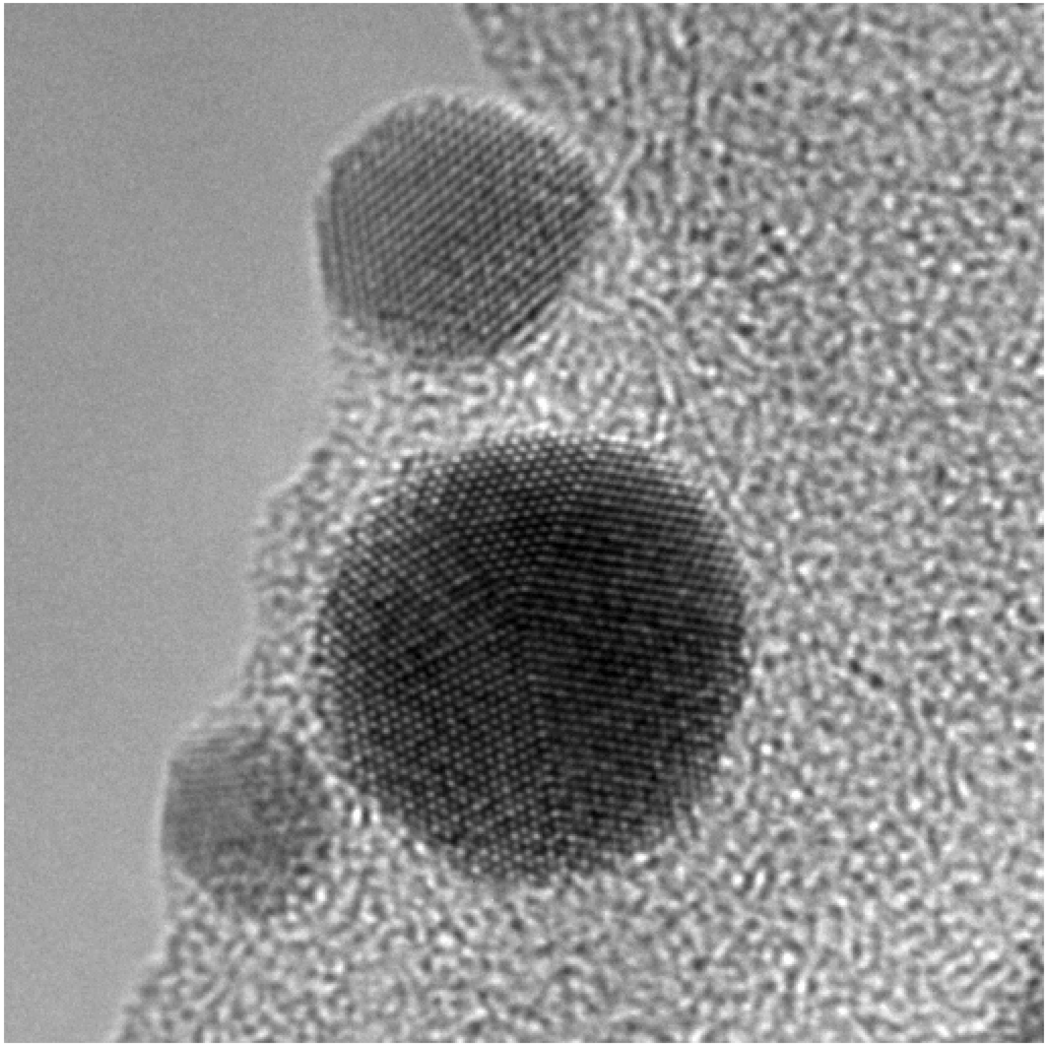

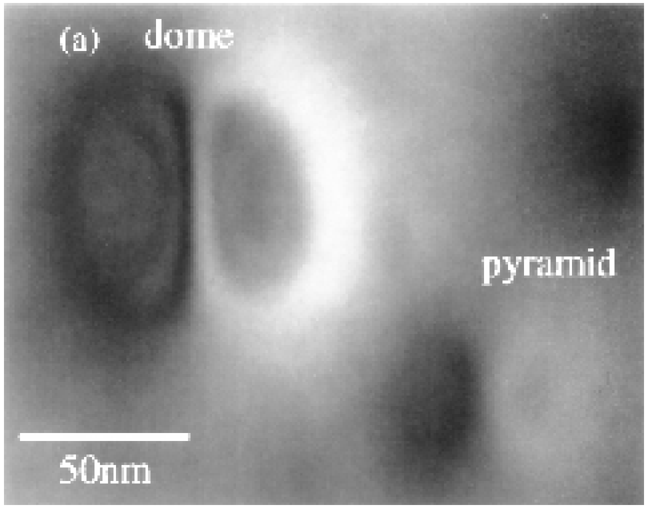

Scanning Probe Microscopy

Atoms moving on a silicon surface

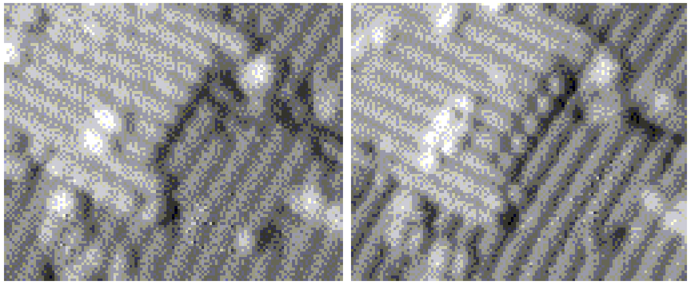

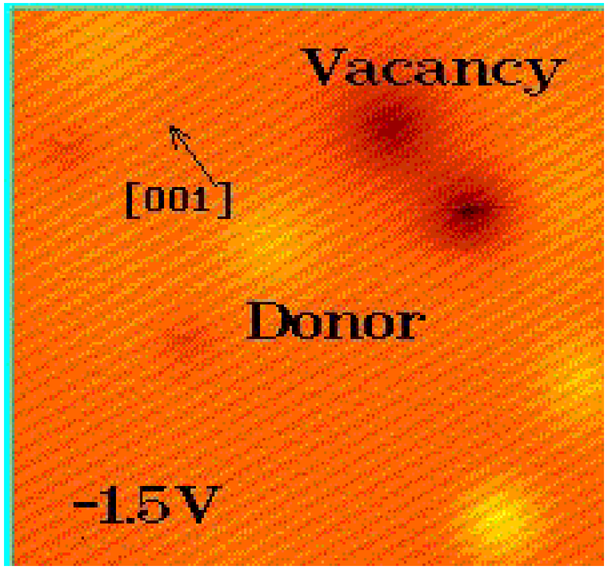

Imaging electronic states from
dopants and imperfections
in semiconductors

New Probes..

e.g. Magnetic Force Microscopy of a Hard Disk

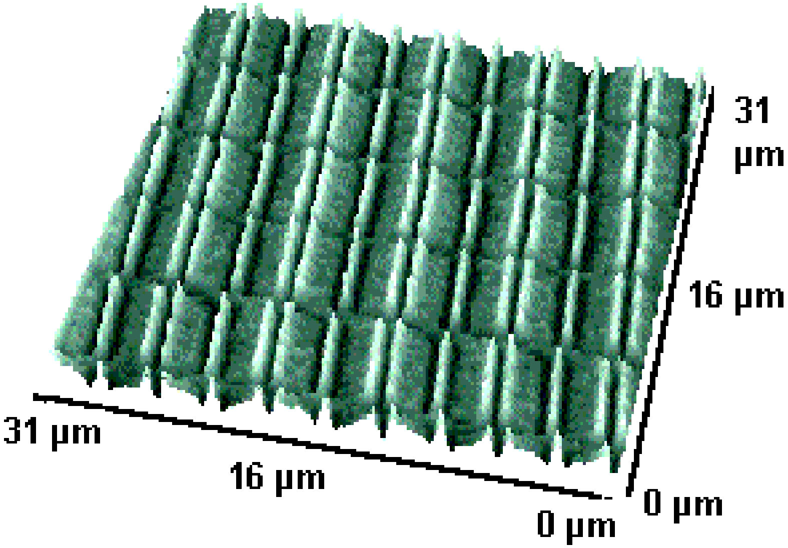

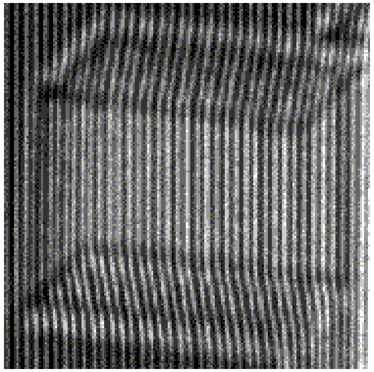

Related magnetic imaging - SEMPA, TEM Holography

Mosquito head and compound eye

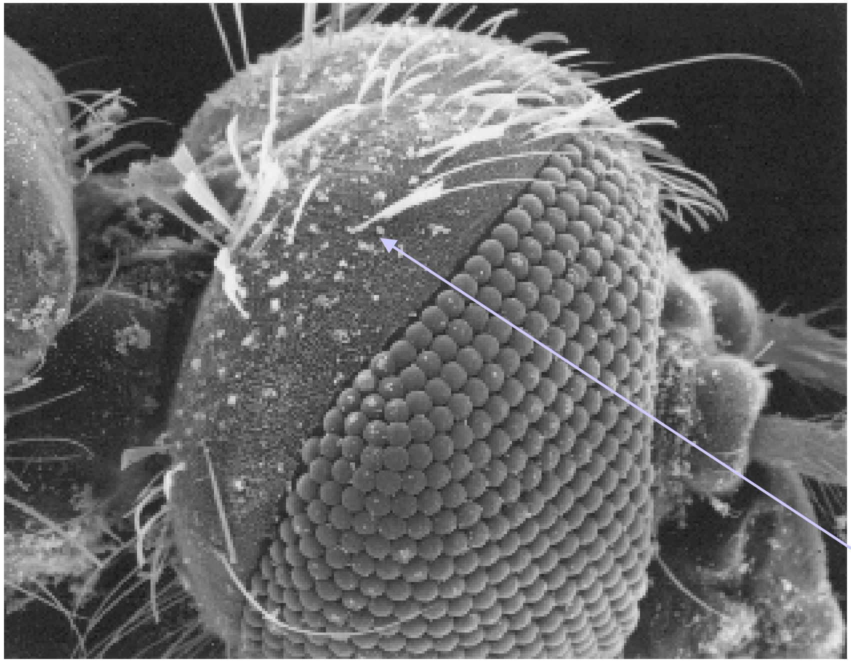

Surface - “no” diffraction

1 μ m

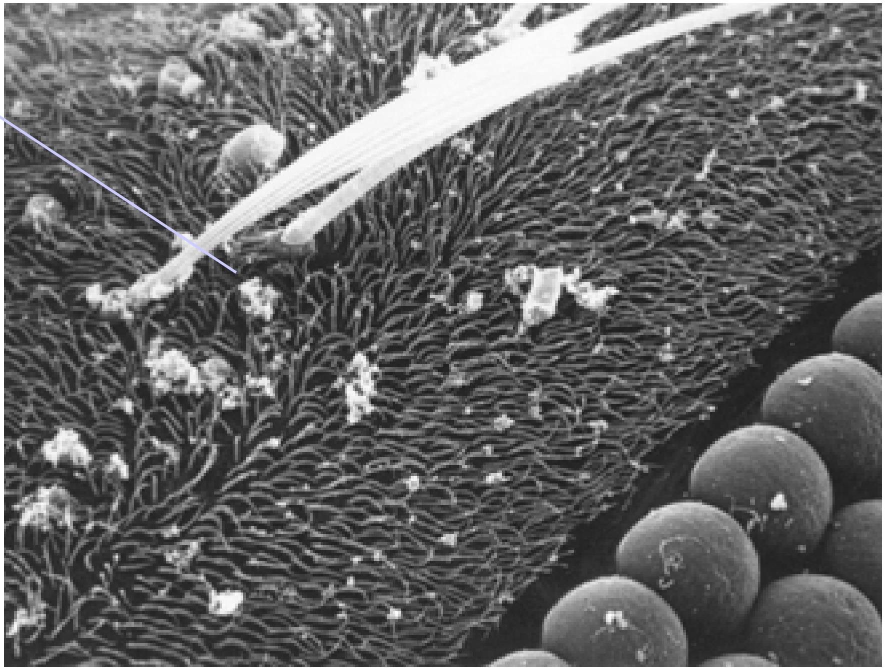

note depth of field

Scanning
Electron
Microscopy

US Electron Beam Microcharacterization Facilities

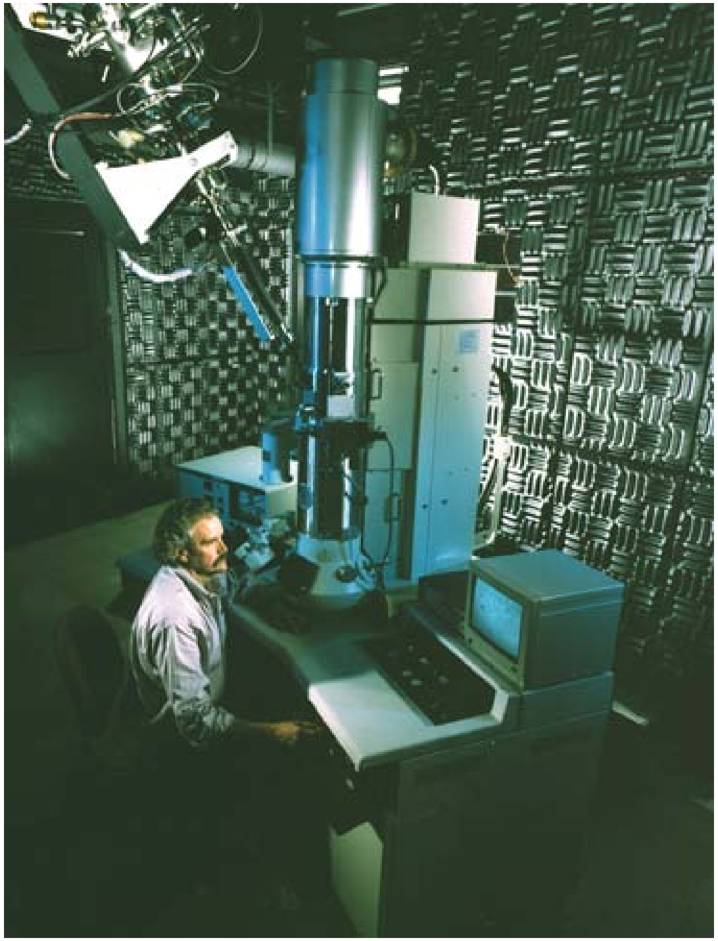

Argonne National Lab

4 DOE National Centers
-specialized techniques
-new aberration correction project - TEAM

26 NSF MRSEC Centers
- broad central facilities

~100 other smaller centers
- typically single instrument

X-Ray Microscopy

- **Hard x-rays focused to 30 nm ("Nanoprobe")**
  - Nanoscale strain measurement
  - Imaging of domains, *e.g.,* in ferroelectrics
  - Magnetism
  - Fluorescence spectro-microscopy
- **Aiming at sub 10nm resolution**
- **Now operating jointly with the Center for Nanoscale Materials at ANL**

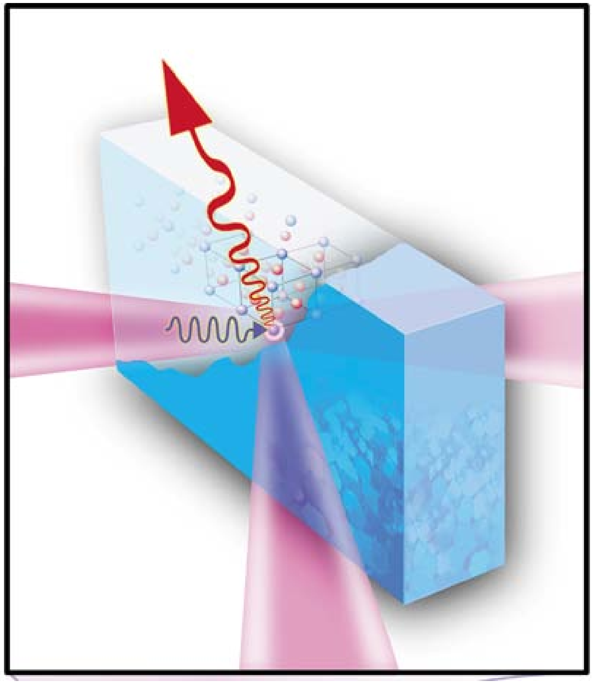

Electron Scattering

$$f_x(\underline{k}) = \iint \rho(\underline{r}) e^{i\underline{k}\bullet\underline{r}} d^3 r \qquad f_{el}(\underline{k}) = \iint V(\underline{r}) e^{i\underline{k}\bullet\underline{r}} d^3 r$$

$$\nabla^2 V(\underline{r}) = -\rho(\underline{r}) / \varepsilon_0$$

$$f_{el}(\underline{k}) = a \frac{(Z - f_x)}{k^2}$$

Mott Formula

Atom Form Factors

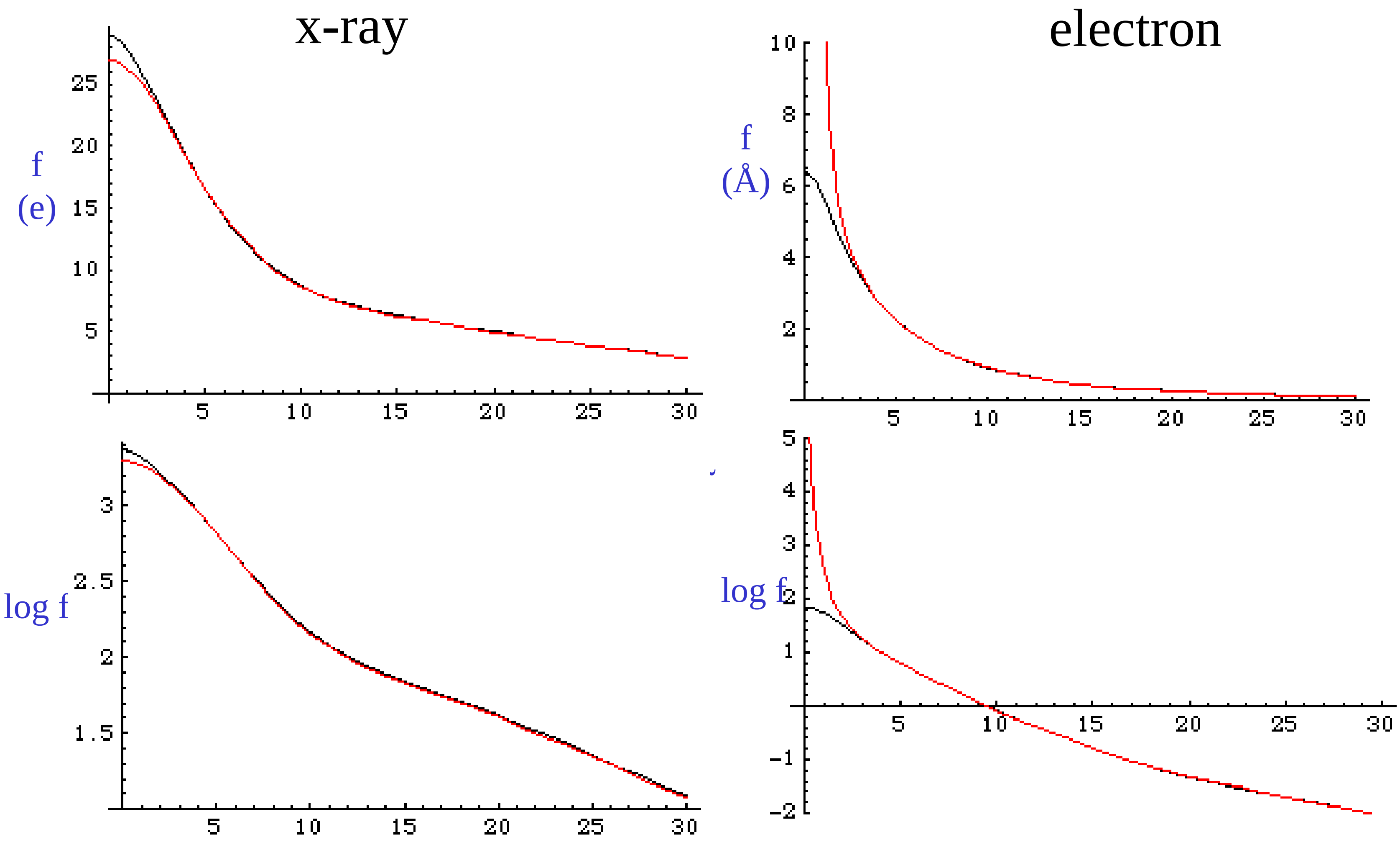

Sensitivity of form factors to charge

d spacing (Å)	*change in f_x (%)*	*change in f_{el} (%)*
2	-0.7	2.1
4	-3.4	32.3
8	-5.7	199.0

What the particle sees….

$\rho_e(\underline{r})$ $V(\underline{r})$ m_n, $\underline{J}$

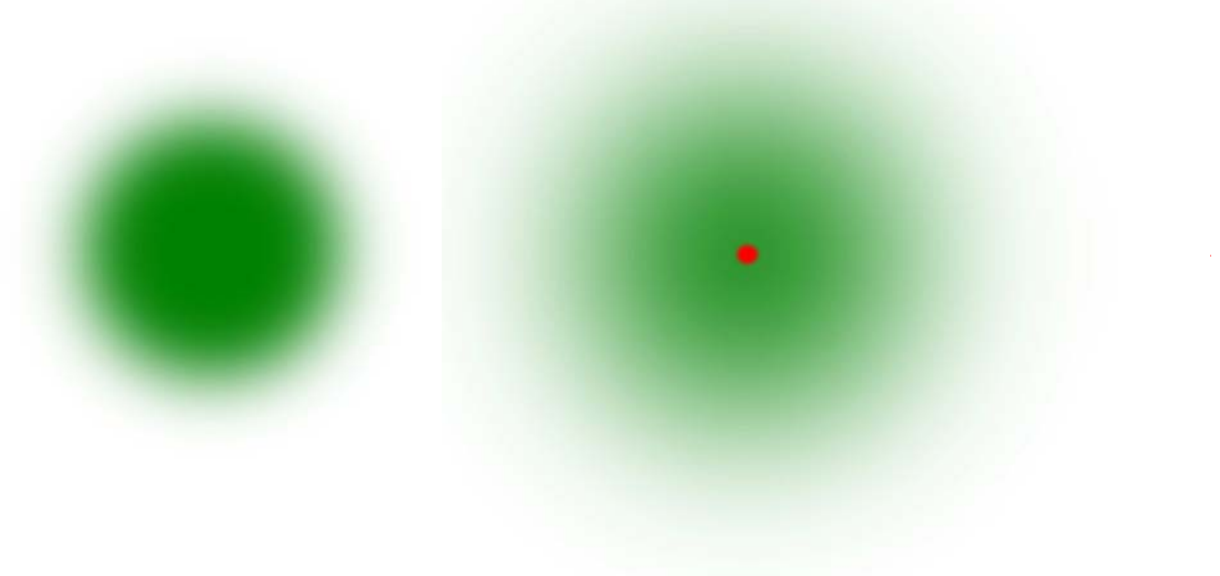

x-ray electron neutron

Electron Form Factors

- Similar dependence on Z
- At high angles - Rutherford-like

$$f_{el}(k) = a\frac{Z}{k^2}$$

Advantages/Disadvantages

Thermal Neutrons	Synchrotron X-rays	Fast Electrons
$\lambda \sim d_{hkl}$	$\lambda \sim d_{hkl}$	$\lambda << d_{hkl}$
penetrates	high brilliance	high brilliance, nanoprobes
strong contrast possible (e.g. H/D)	no kinematic restrictions	no kinematic restrictions
E~elementary excitations	no ΔE restriction	no ΔE or ΔQ restriction
strong magnetic scattering		charge sensitive
		thin samples (or surfaces)
low brilliance	strong absorption at low E	dynamical scattering
some elements absorb strongly	little contrast e.g. H-C	little contrast e.g. hydrocarbons
restrictions on Q for large ΔE	weak scattering from light elements	weak scattering from light elements
excitations < 100meV	radiation damage	radiation damage

← courtesy Sunil Sinha →

Complementarity of techniques

Radiation	*Source Brightness (particles/cm^2/steradian/eV)*	*Elastic Mean-Free Path (Å)*	*Absorption Length (Å)*	*Minimum Probe Size (Å)*
Neutrons	10^{14}	10^{8}	10^{9}	10^{7}
X-rays	10^{26}	10^{4}	10^{6}	10^{3}
Electrons	10^{29}	10^{2}	10^{3}	1

Electron Diffraction

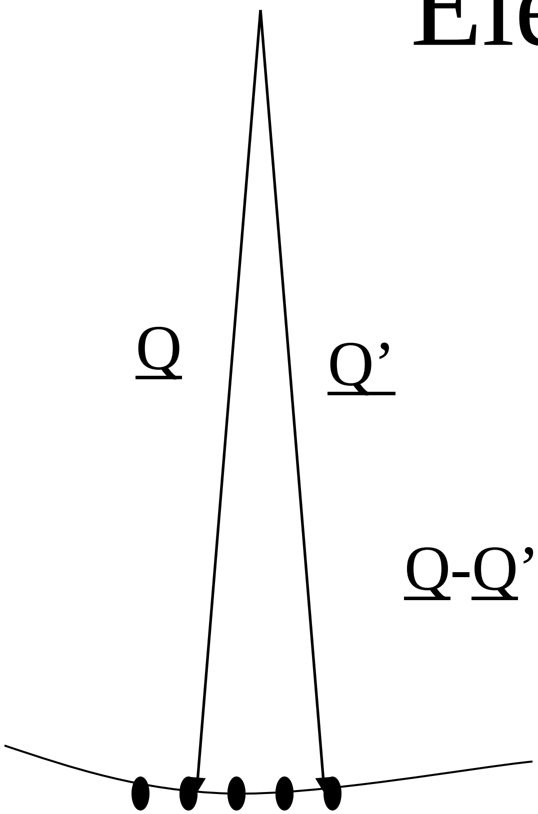

$\underline{Q}-\underline{Q}'=g$

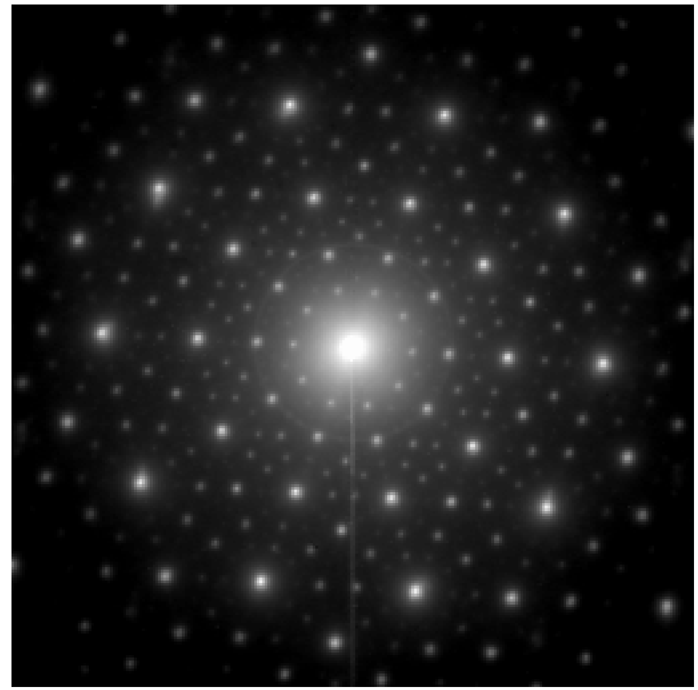

Ewald sphere "flat"

Kinematic theory c.f. x-rays/neutrons

predicts diffraction pattern geometry, qualitative effects

Dynamical Theory of Diffraction

$$\frac{d\phi_0}{dz} = \frac{i\pi}{\xi_0}\phi_0 + \frac{i\pi}{\xi_g}\phi_g e^{2\pi isz}$$

$$\frac{d\phi_g}{dz} = \frac{i\pi}{\xi_g}\phi_0 e^{-2\pi isz} + \frac{i\pi}{\xi_0}\phi_g$$

2-beam theory can
be extended to N beams
- BLOCH WAVES

Extinction distance: $\zeta_g = \frac{\pi\Omega}{\lambda F}$

typically ~1000 Å
at 100kV

absorption is added as an imaginary extinction

Convergent Beam Electron Diffraction

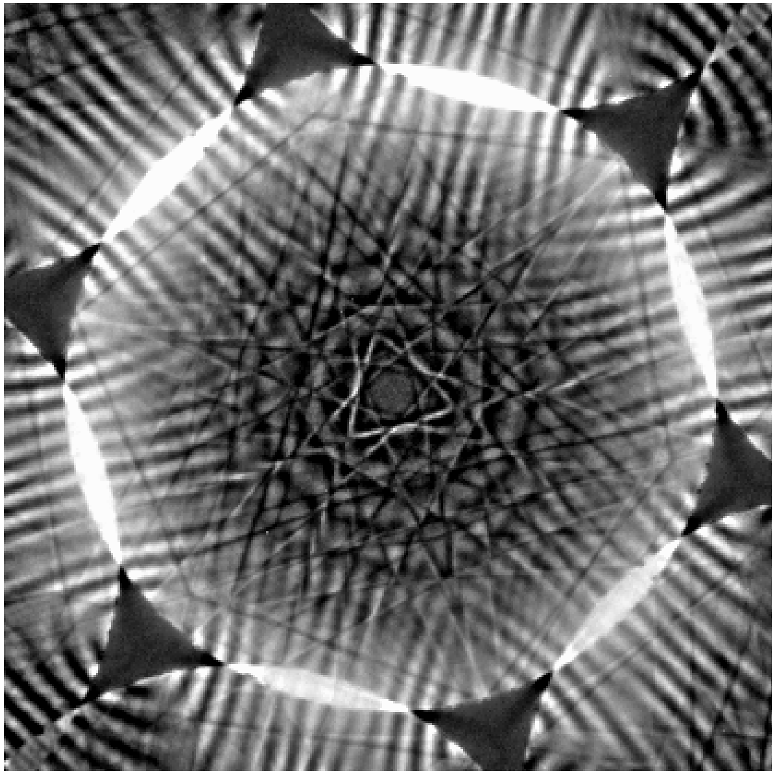

Si (111)

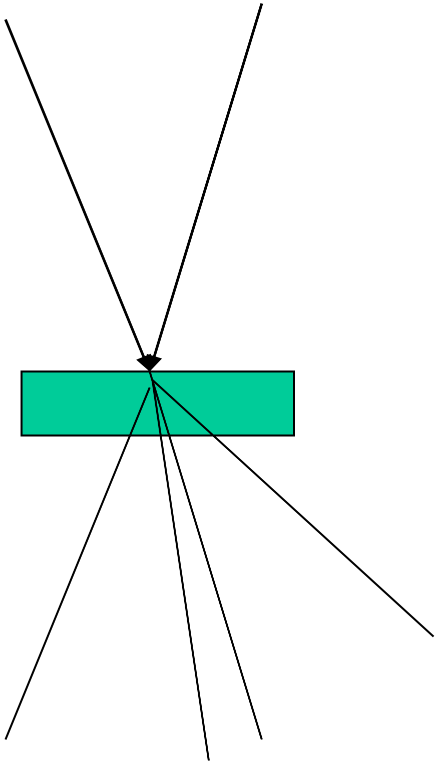

reveals full symmetry

Imaging

The column approximation:

$$\frac{d\phi_0}{dz} = \frac{i\pi}{\xi_0}\phi_0 + \frac{i\pi}{\xi_g}\phi_g e^{2\pi i(sz + \underline{g}\bullet d\underline{R}/dz)}$$

$$\frac{d\phi_g}{dz} = \frac{i\pi}{\xi_g}\phi_0 e^{-2\pi isz} + \frac{i\pi}{\xi_0}\phi_g$$

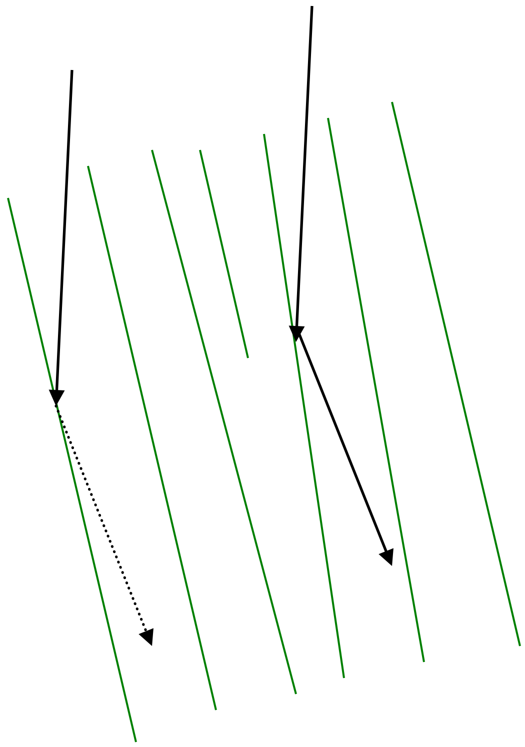

edge dislocation

displacement field $\underline{R}$

Howie-Whelan Equations

predicts strain-contrast images well at ~20Å resolution

Multi-slice theory

More accurate but less-efficient approximation
propagates electrons between thin (kinematical) slices

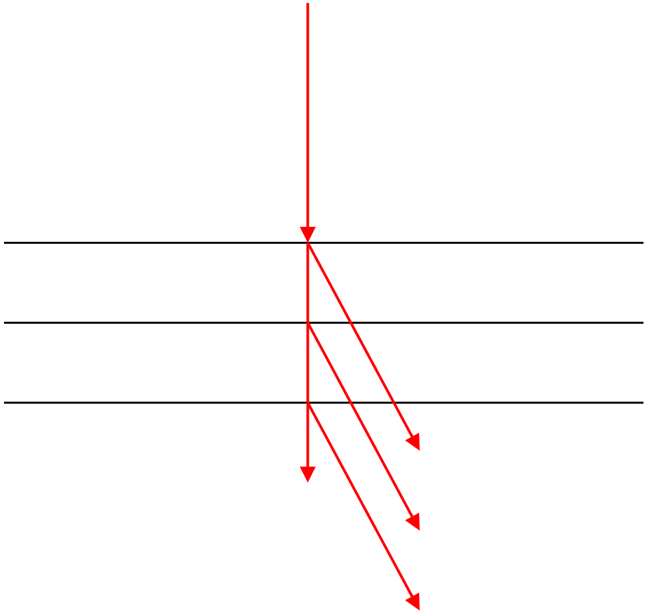

includes many-beam effects and fresnel propagation

appropriate for high-resolution (<5Å) imaging

Fourier Optics

- Diffraction and Imaging
  - Fraunhofer diffraction $F(\underline{Q}) = \iint \phi(\underline{r}) e^{i\underline{Q}\bullet\underline{r}}$
    - one fourier transform
  - Imaging (with a lens) $\varphi(\underline{r}) = \iint F(\underline{Q}) e^{-i\underline{Q}\bullet\underline{r}}$
    - Second fourier transform

    - It gets interesting when you filter in one space or the other

Simple Consequence

- Abbe's theory of the microscope resolution

$$\varphi(\underline{r}) = \iint A(\underline{Q})\, F(\underline{Q})\, e^{-i\underline{Q}\bullet\underline{r}}$$

=convolution with F.T. (A)

– and the Rayleigh Criterion

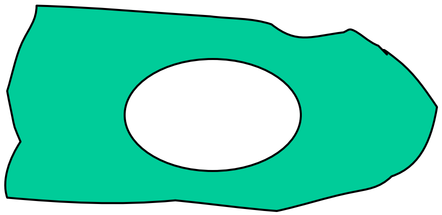

Aperture in focal plane

A(Q) = 1; $Q < Q_0$

A(Q) = 0; $Q > Q_0$

$$PSF = \frac{2J_1(Q_0 r)}{Q_0 r}$$

$$\Delta = \frac{1.22}{Q_0}$$

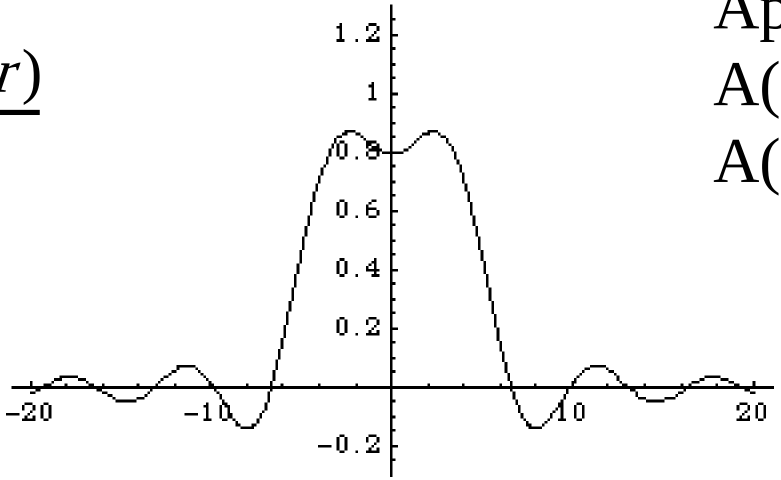

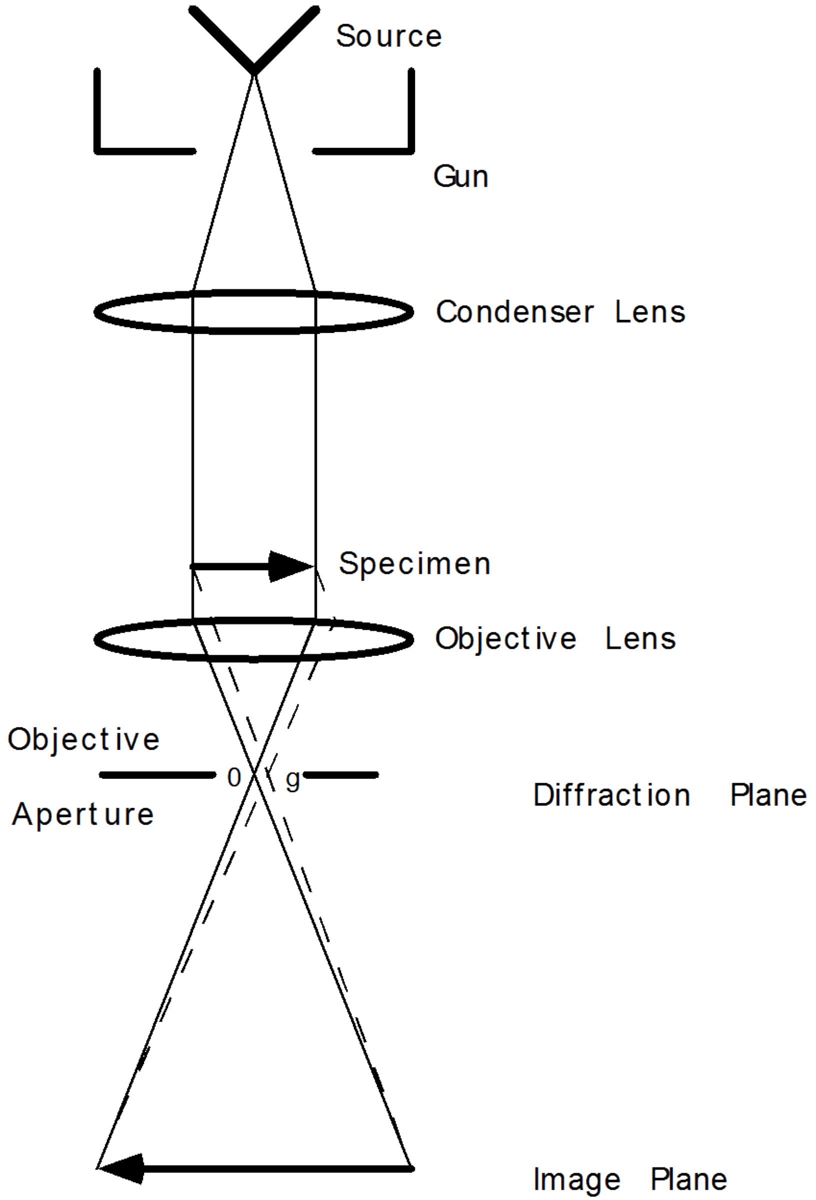

Bright and Dark Field Imaging

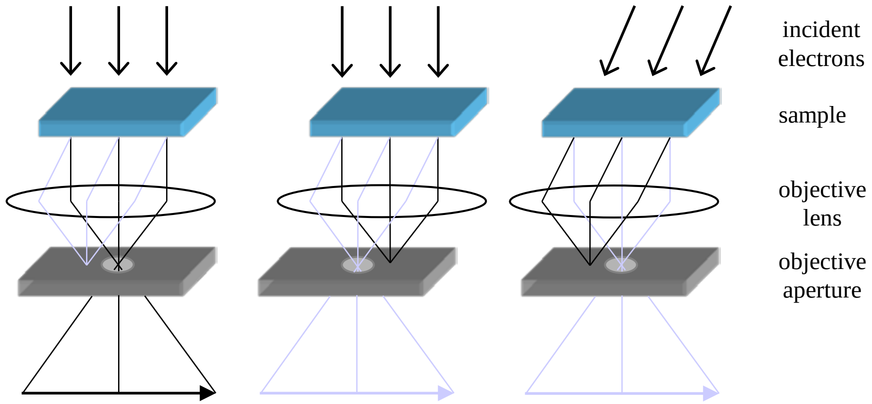

(a). bright field image (b). dark field image (c). tilted dark field image

A 2-D Perfect Crystal?

and it's diffraction pattern

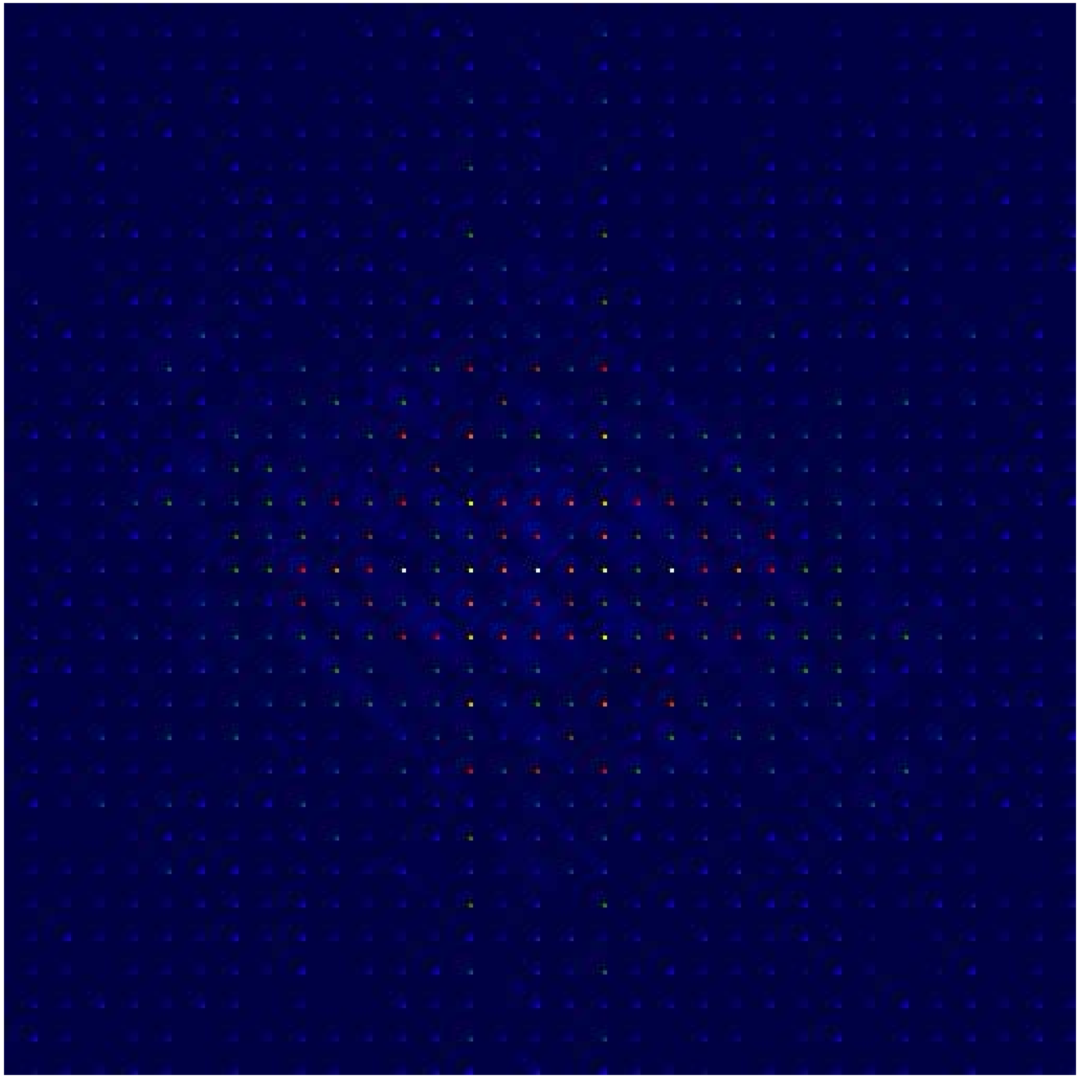

Dark-field image

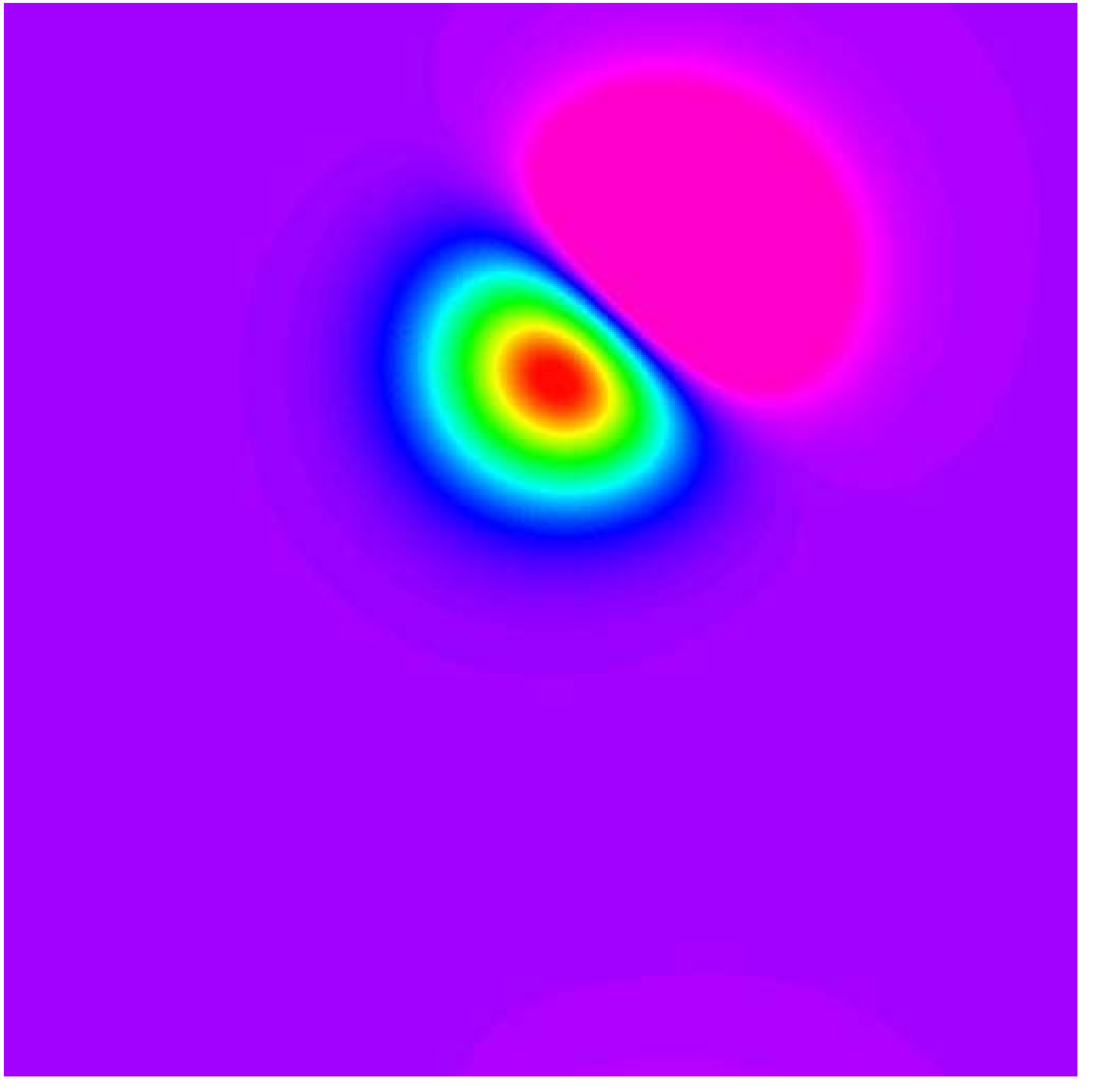

The point defect...

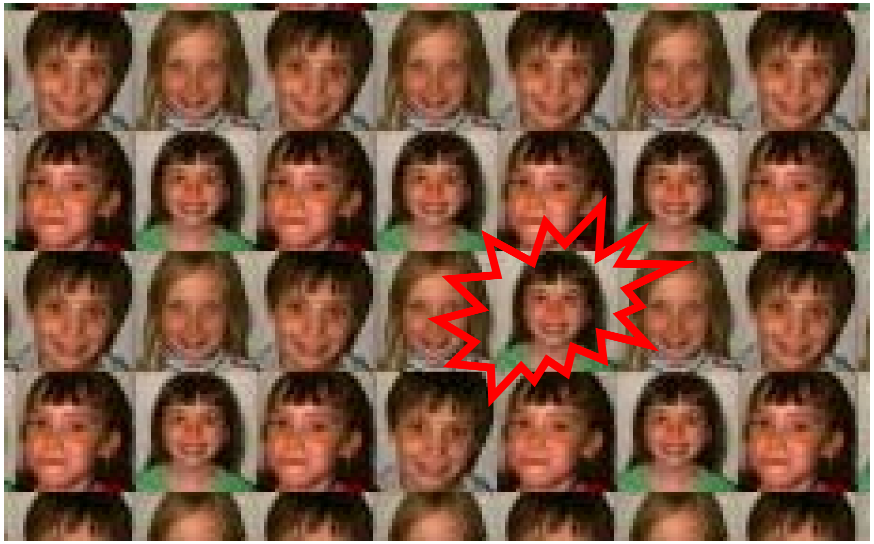

“High-resolution image”

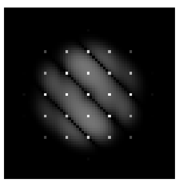

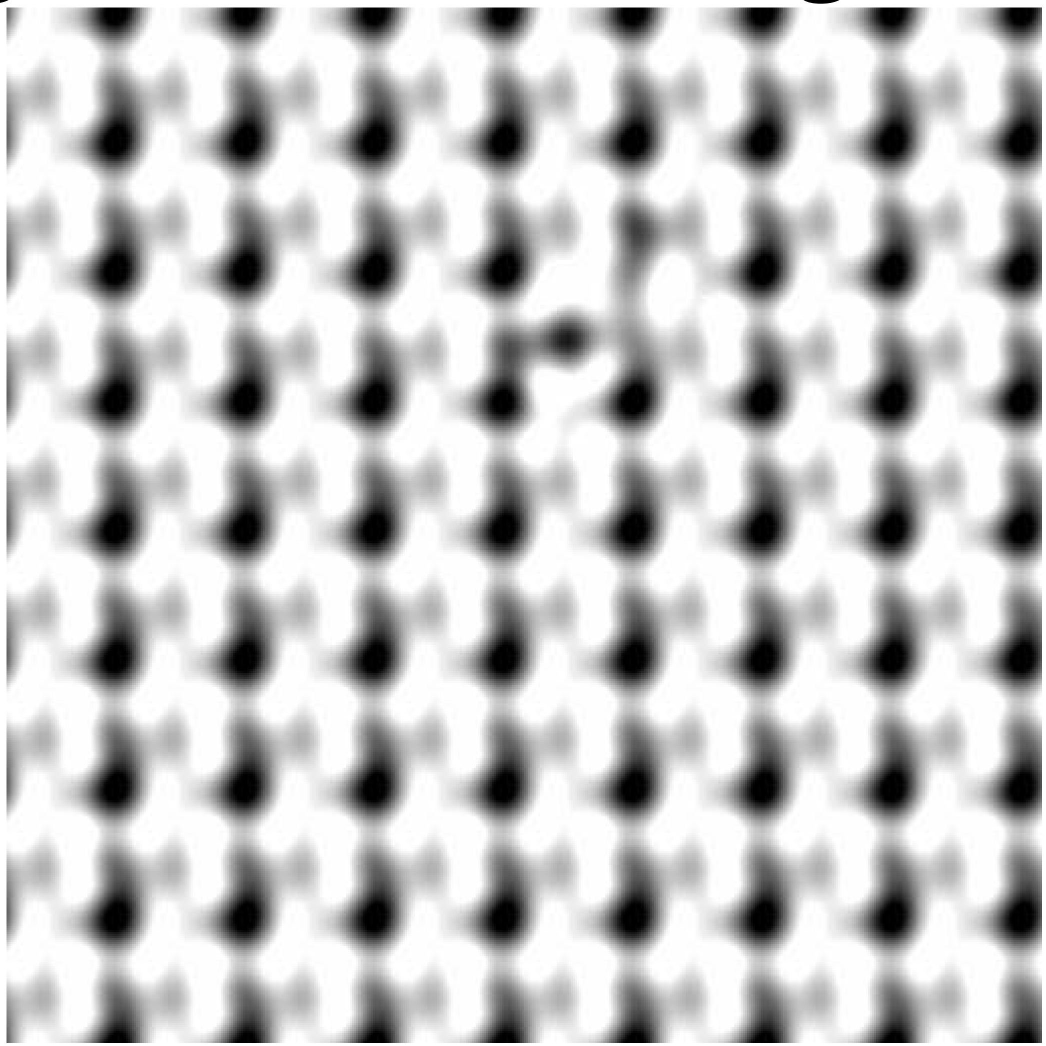

Amplitude Contrast Imaging

Cu_2O Reflection

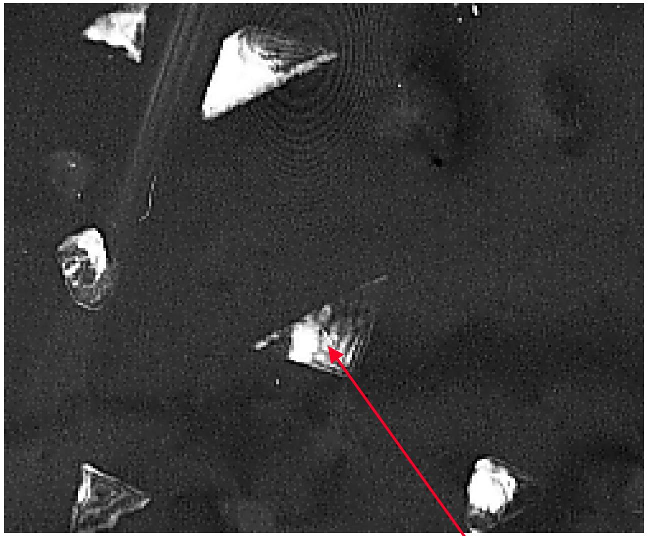

Cu Reflection

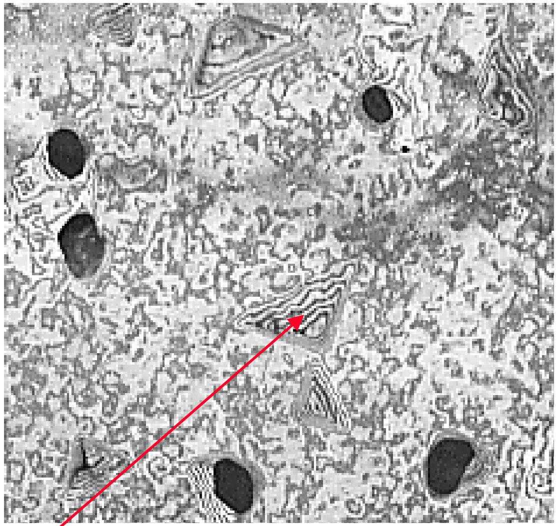

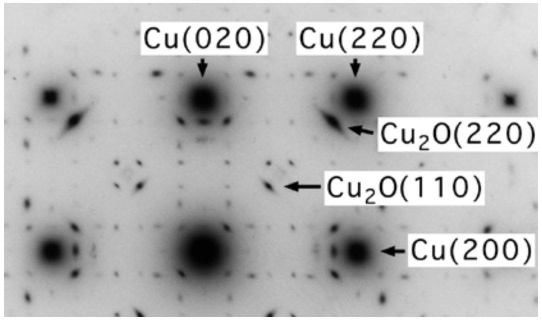

Mixed phase system..

same island

Self-limiting oxidation of copper
Yang, JC; Kolasa, B; Gibson, JM, APPLIED PHYSICS LETTS, **73,** 2841 (1998)

Scanning Transmission Electron Microscopy

“Z-Contrast” STEM

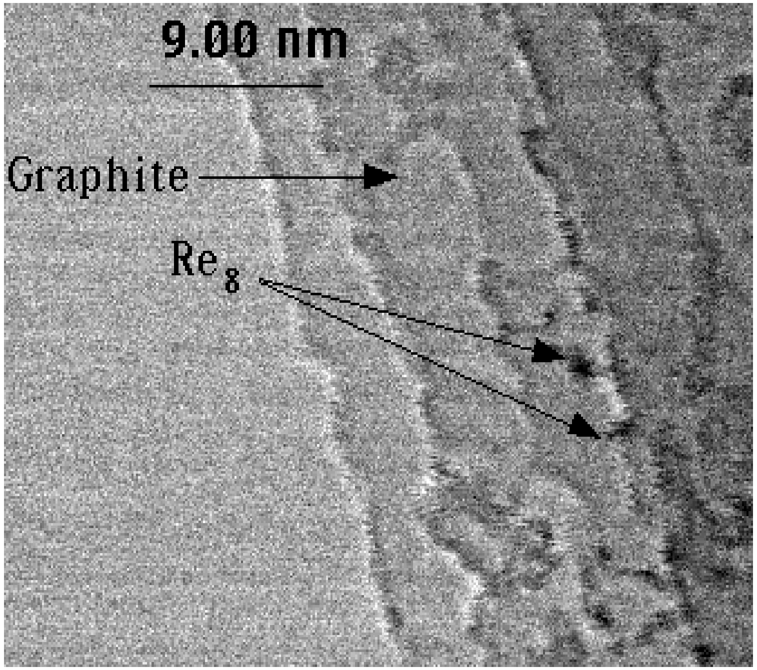

Bright-field STEM Image

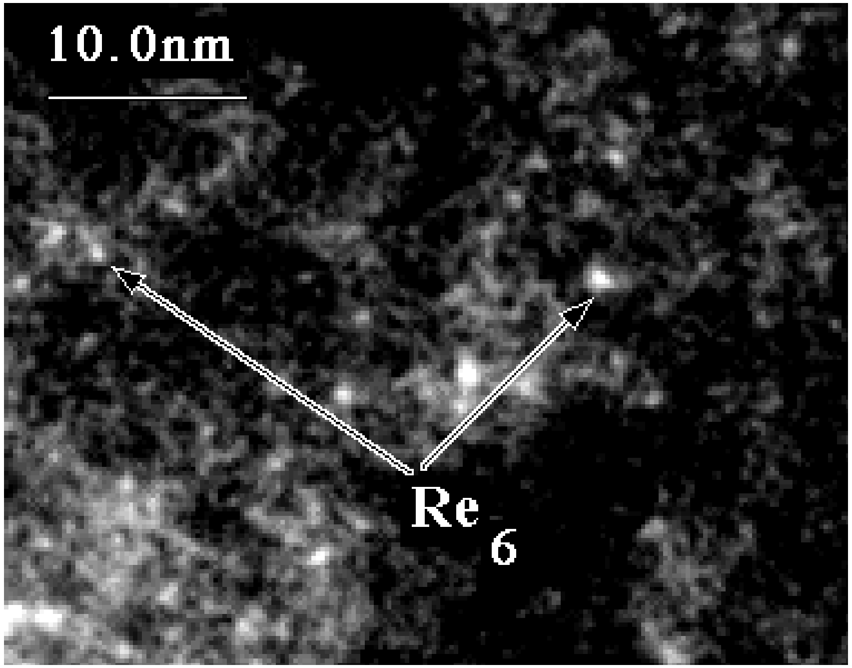

High-angle ADF dark-field image

The principle of reciprocity..

Stability of supported organometallic clusters probed by a mass-sensitive TEM technique
Singhal, A; Gibson, JM; Treacy, MMJ, JOURNAL OF PHYSICAL CHEMISTRY **100** 6385 (1996)

Phase Contrast and High Resolution

- To image lattice resolution < d
  - => $Q_0 > g$ so no amplitude contrast

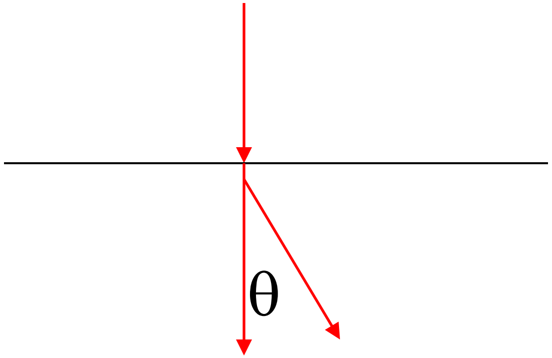

fresnel phase shift ~ $\pi/\lambda\, z\theta^2$

assume object is weak phase shift
(kinematical theory)

$$\psi = e^{i\sigma V(\underline{r})} \approx 1 + i\sigma V(\underline{r})$$

You want a phase shift near -π/2 (Zernicke phase contrast)

Phase shift with aberrations

Phase shifting function (should be near -π/2)

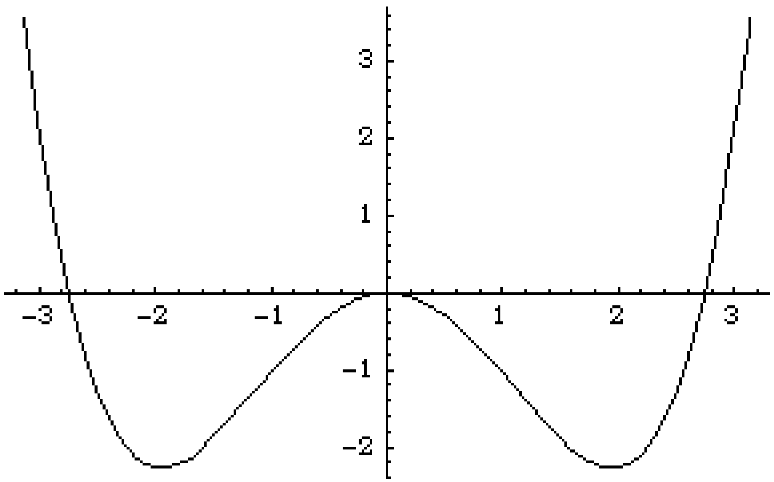

$$\gamma = \pi \lambda (z k^2 + C_s k^4 / 2)$$

$$k = \frac{q}{2\pi}$$

C_s is the spherical aberration coefficient

Ideal defocus (Scherzer) $z = -1.2\sqrt{C_s \lambda} \quad \Rightarrow \quad r = 0.67(C_s \lambda^3)^{1/4}$

point-to-point resolution

State of the art high-resolution

GaN (LBL)

this picture shows reconstructed electron wavefunction revealing split Ga/N atoms

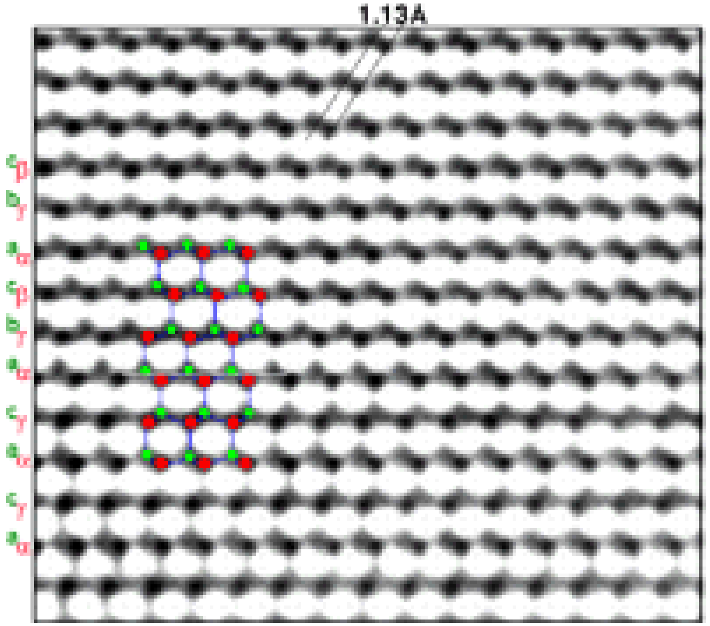

removing the microscope aberrations - wavefront reconstruction, aberration correction

Phase Contrast X-Ray Imaging

Big bugs, Socha et al.,
PNAS **104**, 13198, (2007)

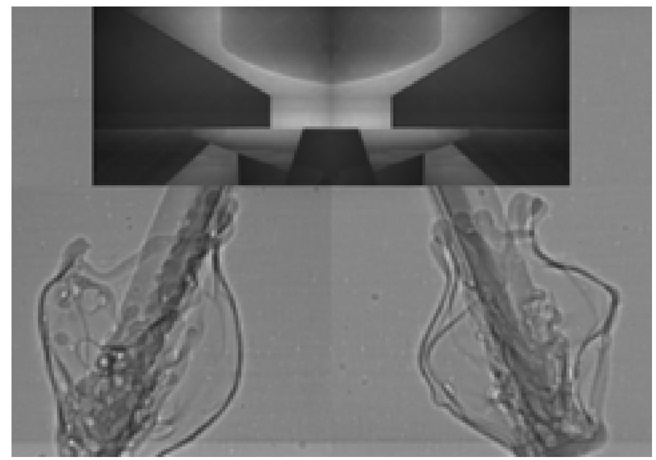

Fuel Sprays: Wang, YJ et al.
NATURE PHYSICS,
4 305 (2008)

Examples

Quantitative determination of local structure and charge distribution in copper oxide

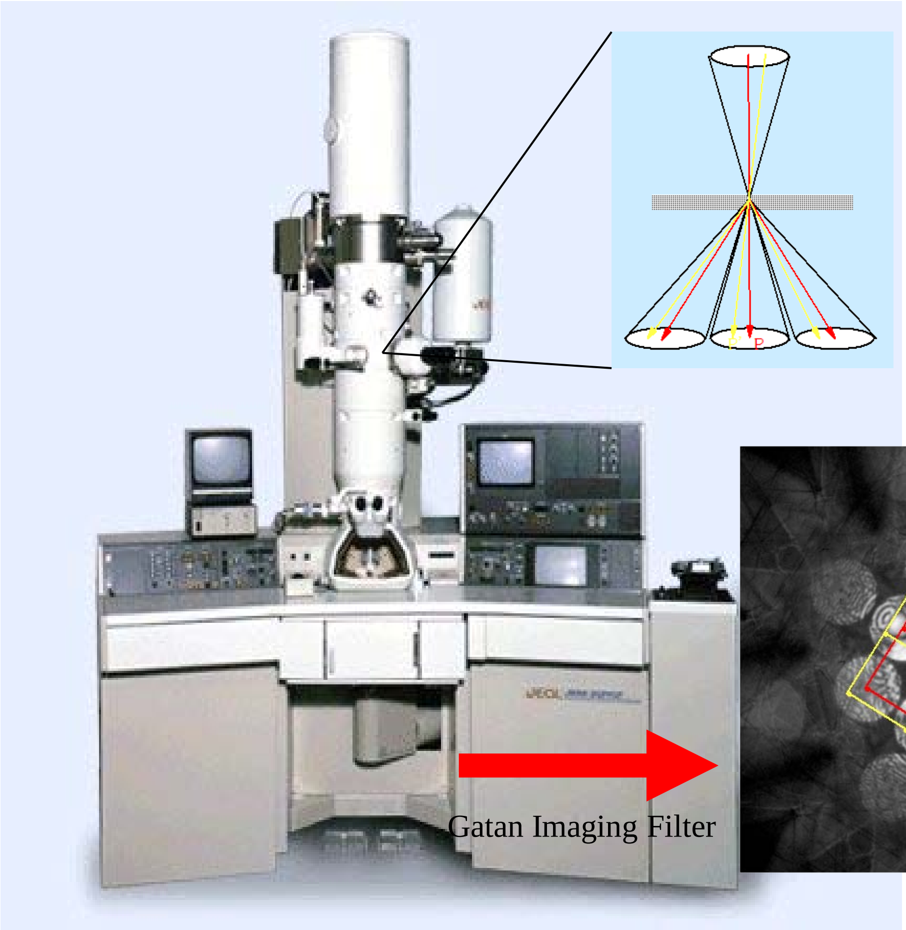

To study :

- Charge and charge states in complex oxides

Using Electron sensitivity to crystal bonding
- combined with x-ray higher order SF accuracy

•Probe formation allows local study

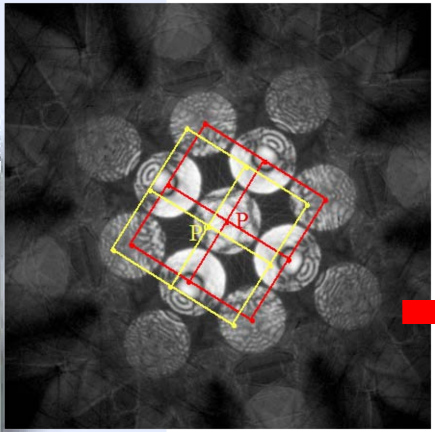

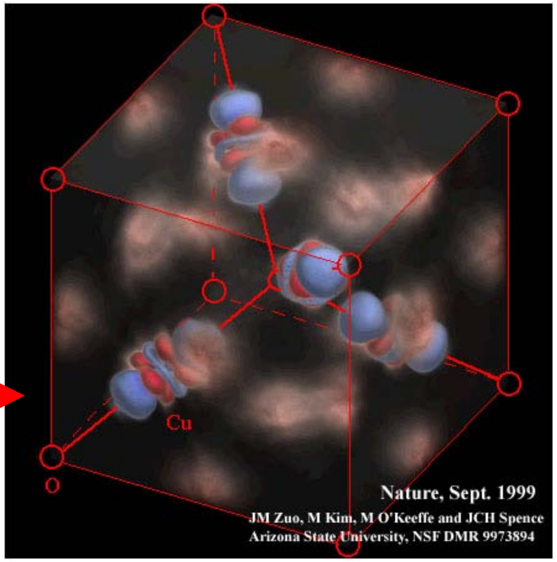

J.M. Zuo and Spence

d-orbitals visualized

Crystallites in glass

- Recent experience with IPNS experiment
- Thermal poling of SiO_2 induced optical nonlinearity
  - Initial IPNS data suggested structural change in amorphous material (Cabrillo, Gibson, Johnson, Bermejo et. al.)
- TEM shows ~5% small crystallites (critobalite)

unpoled

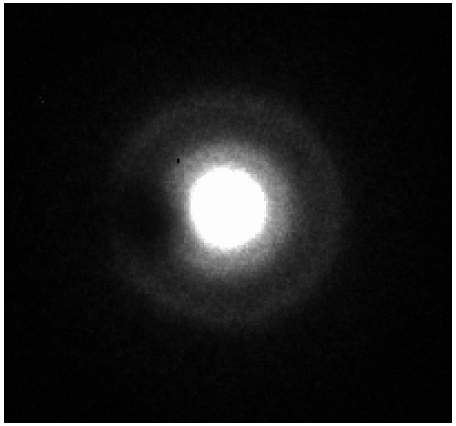

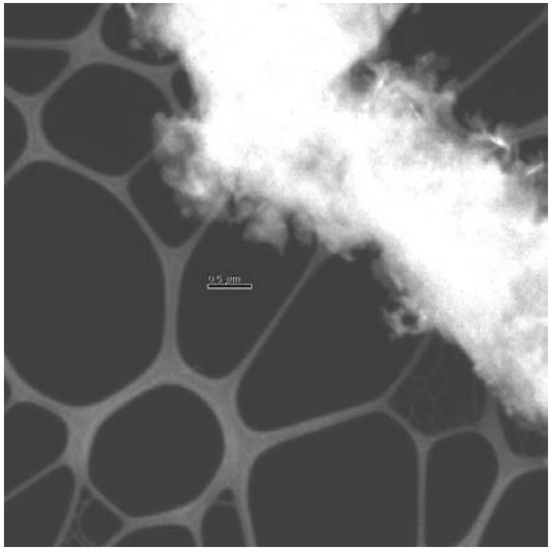

poled

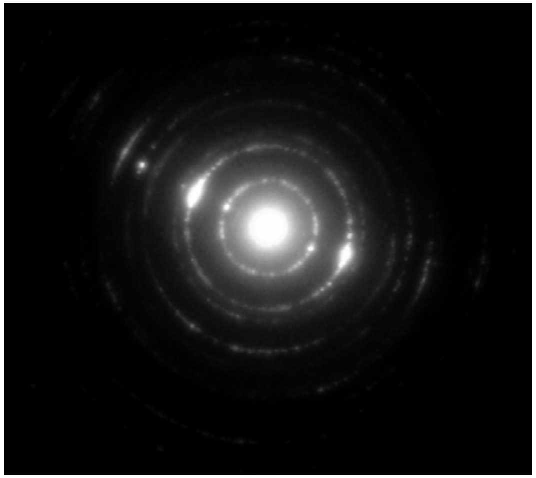

Role of microscopy in confirming homogeneity

APPLIED PHYSICS LETTERS VOLUME 73, NUMBER 19 9 NOVEMBER 1998

Self-limiting oxidation of copper

J. C. Yang,[a] B. Kolasa, and J. M. Gibson
Materials Research Laboratory, University of Illinois at Urbana-Champaign, Urbana, Illinois 61801

M. Yeadon
Institute of Materials Research and Engineering, National University of Singapore, 119260, Singapore

assumes cation drift in uniform film

$$1/h = A - B \ln(t)$$

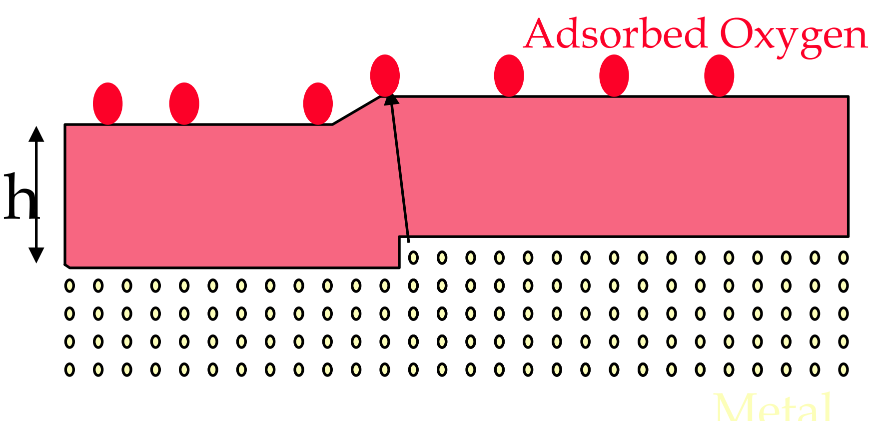

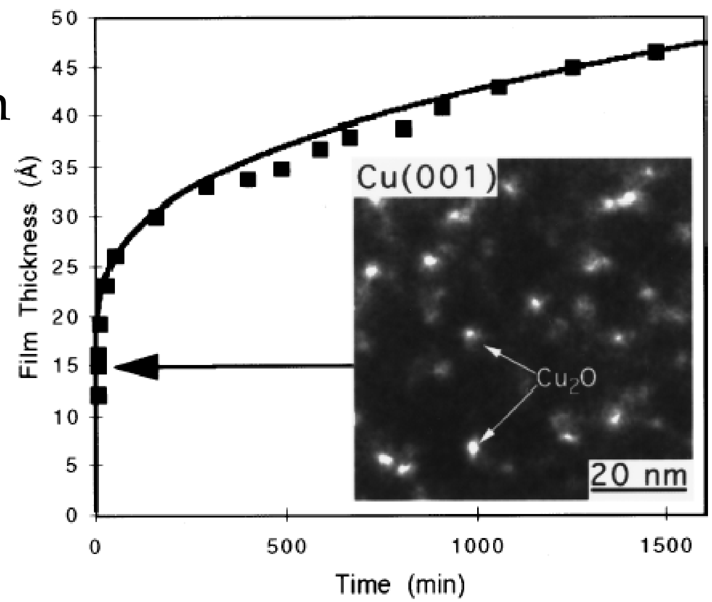

FIG. 1. Oxide thickness Cu_2O of vs time from Young *et al.* (see Ref. 2) of the thickness of the Cu_2O as function of time, when single crystal (001) Cu was oxidized in 760 Torr O_2 at 70 °C. The arrow points to the experimental condition we used. (Inset) Dark field image from the Cu_2O reflection, where the bright specks are Cu_2O islands.

N.Cabrera, N.F. Mott, Rept. Progr. Phys. **12**, 163 (1948)

Dark-field imaging of phases

Cu_2O Reflection

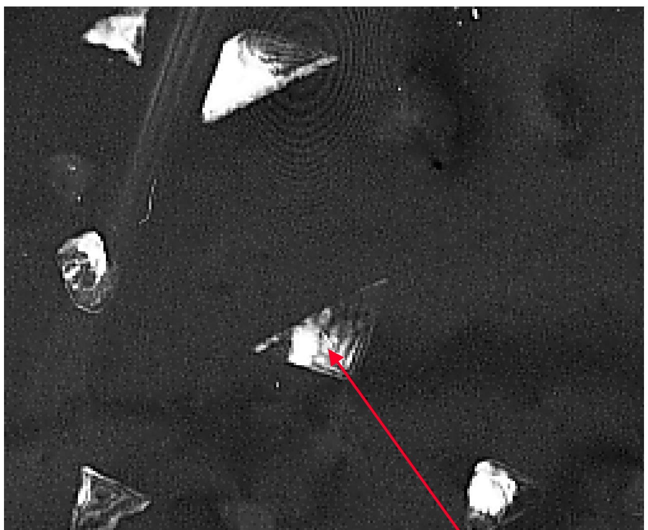

Cu Reflection

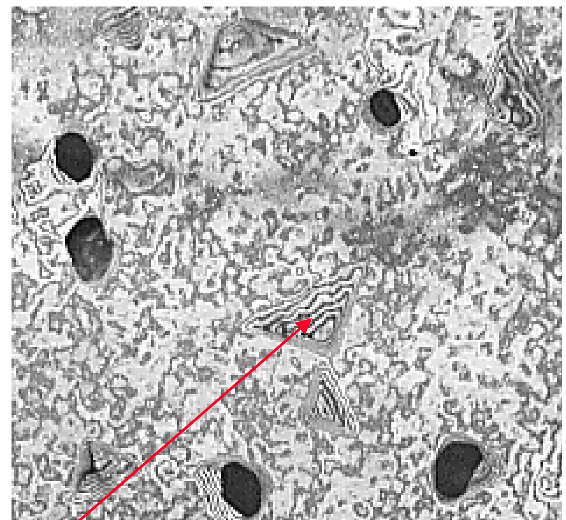

same island

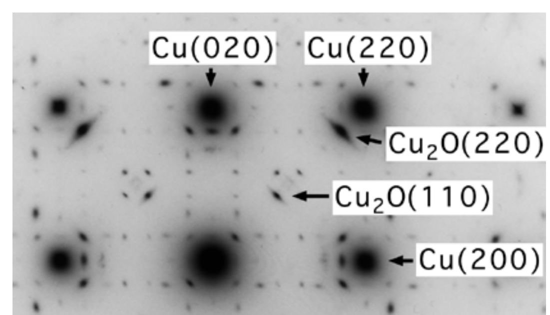

Strain Evolution in Coherent Ge/Si Islands

Chuan-Pu Liu,[1,*] J. Murray Gibson,[1] David G. Cahill,[1] Theodore I. Kamins,[2] David P. Basile,[2] and R. Stanley Williams[2]

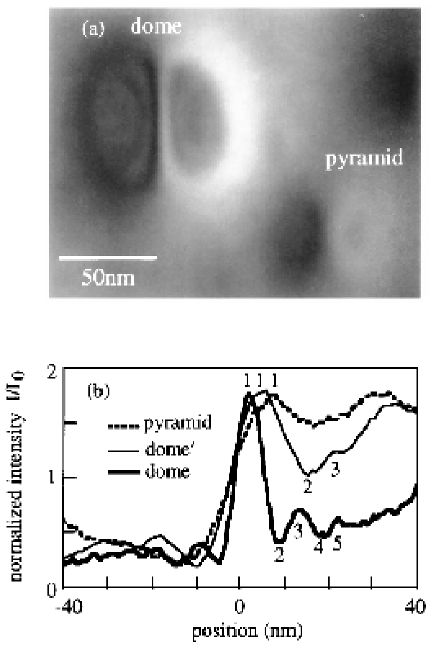

FIG. 1. Dark-field images of a pyramid and a dome using $\mathbf{g} = 400$. (b) Line traces across three typical islands found in the experiment, where the fringes on one side of the images are numbered.

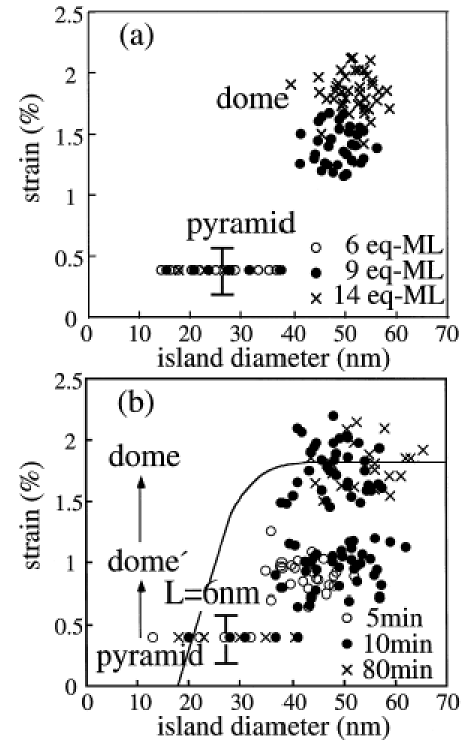

FIG. 2. Strain in Ge islands vs island diameter. (a) For as-deposited samples 6, 9, and 14 eq-ML thick grown at 600 °C and (b) for 8 eq-ML thick samples deposited at 550 °C and annealed at 550 °C for 5, 10, and 80 min. The error ranges both in diameter and strain are 10%. The solid curve in (b) represents the dependence of the island diameter on the strain of equilibrium islands with isotropic surface energies, derived from the work of Kukta and Freund [17] using $L = 6$ nm (see text for details). The island populations in a sample annealed for 40 min are similar to that for 80 min (data not shown).

Defect Imaging

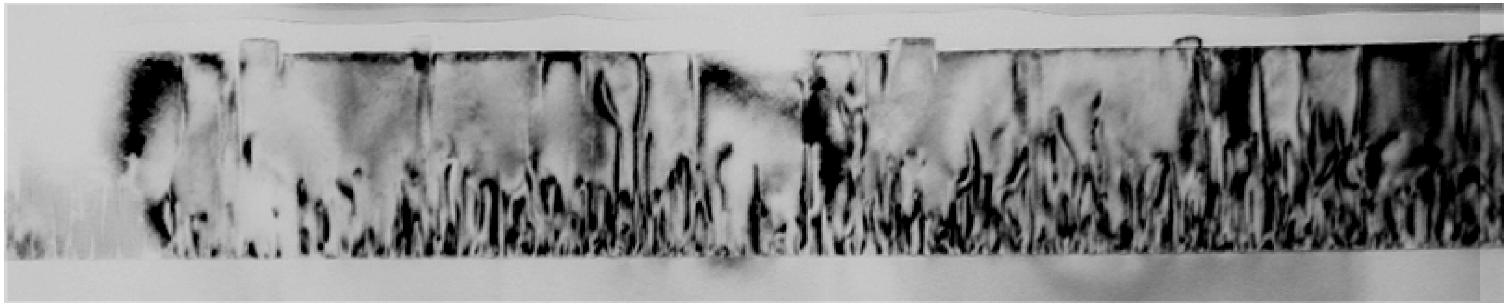

Threading dislocations in GaN

Strain contrast imaging of defects
- allows determination of burger's vector

Density (/cm^2)	10^{14}	10^{12}	10^4
Technique	XRD rocking curve	TEM	X-ray Tomography

Pop. density in Chicago?

High T_c Superconductors

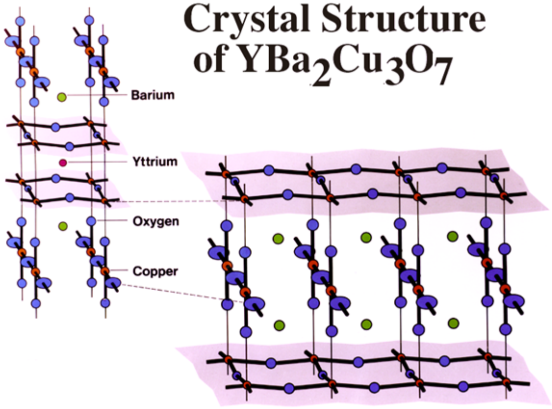

- Neutron Diffraction -
  - crystal structure
- X-Ray Photoemission
  - understand pairing mechanism?
- Transmission Electron Microscopy
  - Thin film structure and defects
  - Grain Boundaries
    - Understand J_c

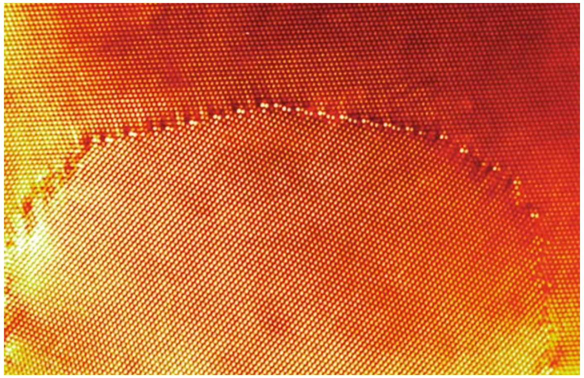

Interface Science

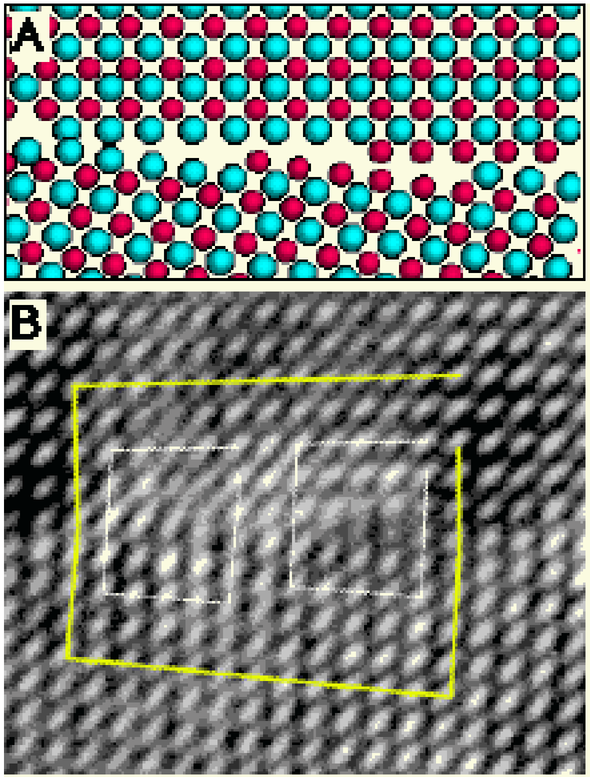

Atomic structure
of grain boundary in zirconia

Merkle ANL

http://www.msd.anl.gov:50610/groups/im/highlights/yszmicroscopy/ysz.html

“Atomic Scale” Spectroscopy

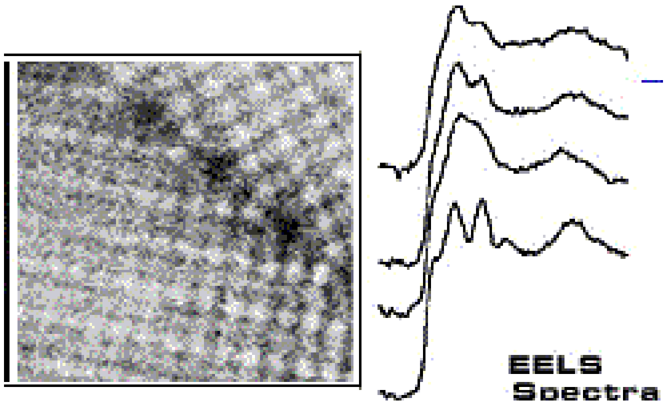

Browning, U. Illinois Chicago

near-edge structure of oxygen near a zirconia boundary

Surface/Interface Roughness

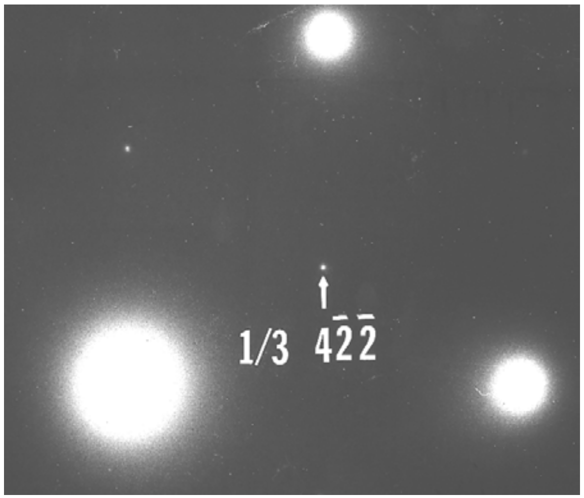

Silicon (111)

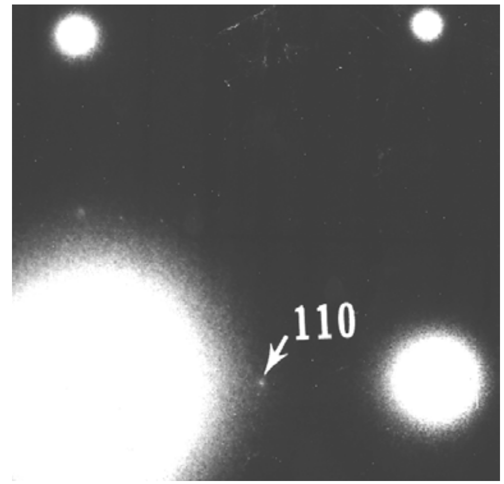

Silicon (100)

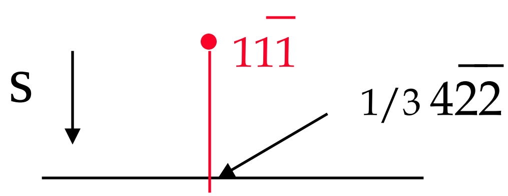

zero-order laue-zone

Crystal Truncation Rods

Chen and Gibson, Phys. Rev. B **54**, 2846 (1996)

Imaging Roughness

s=0.02Å^{-1}

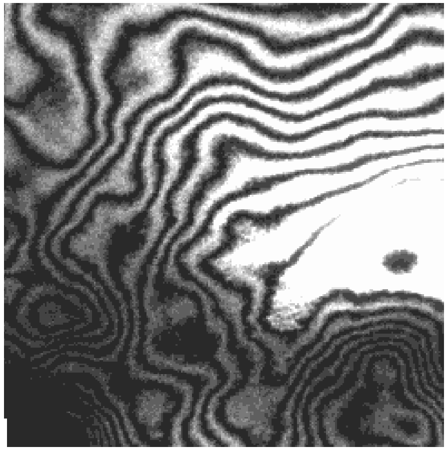

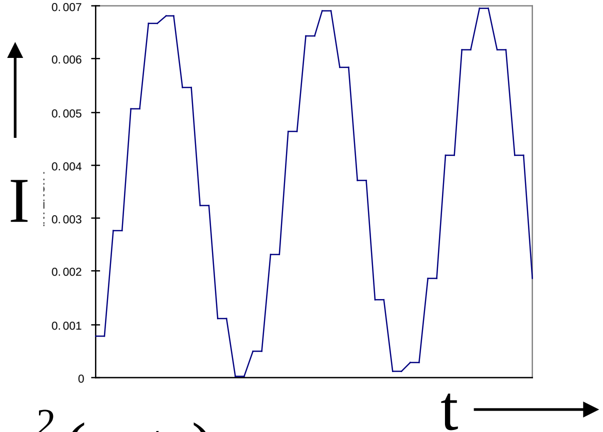

$$I = \frac{1}{s^2 \xi_g^2} \sin^2(\pi t s)$$

s=0.05Å^{-1}

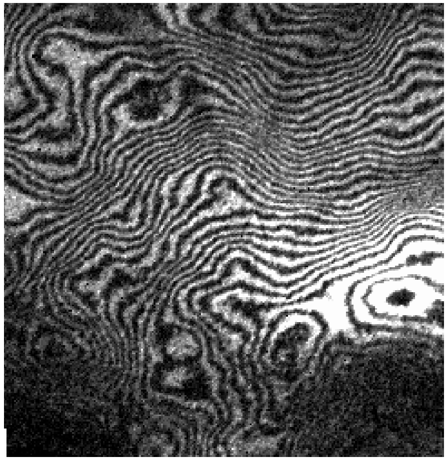

x10

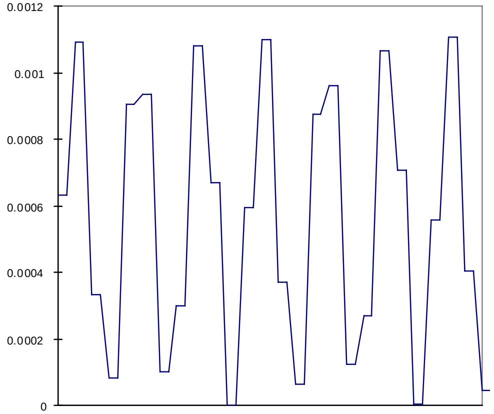

“diffraction contrast” dark field imaging

Transmission Electron Microscopy and Roughness

- familiar in cross-section

  but limited by projection,
  and sampling

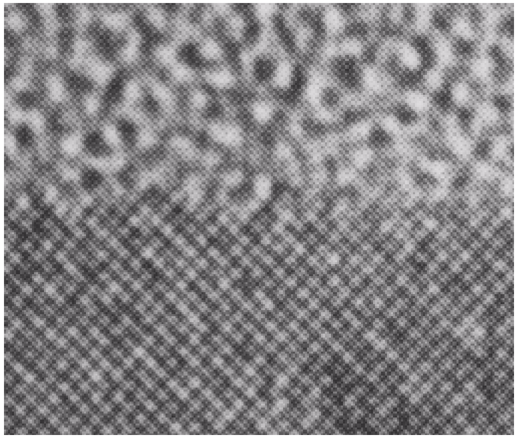

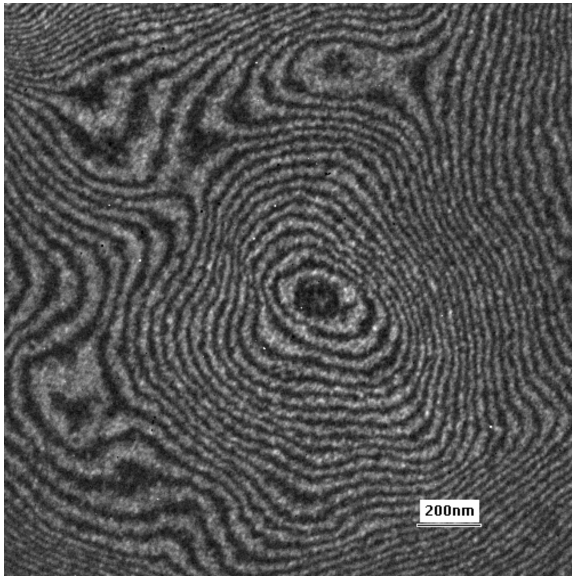

Our method uses plan-view imaging

limited to specially prepared
samples

Earlier work on dynamics of UHV oxidation/etching

SiO formation = etching

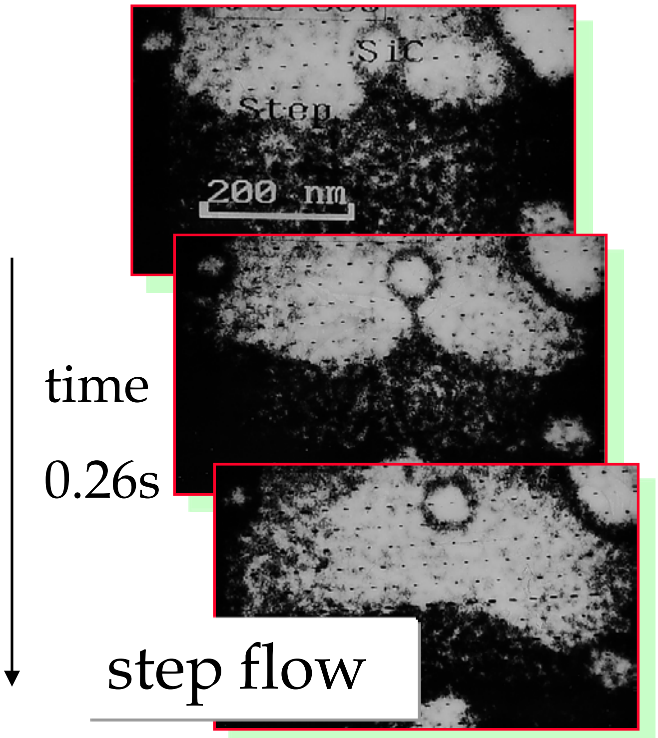

SiO_2 formation = oxide growth

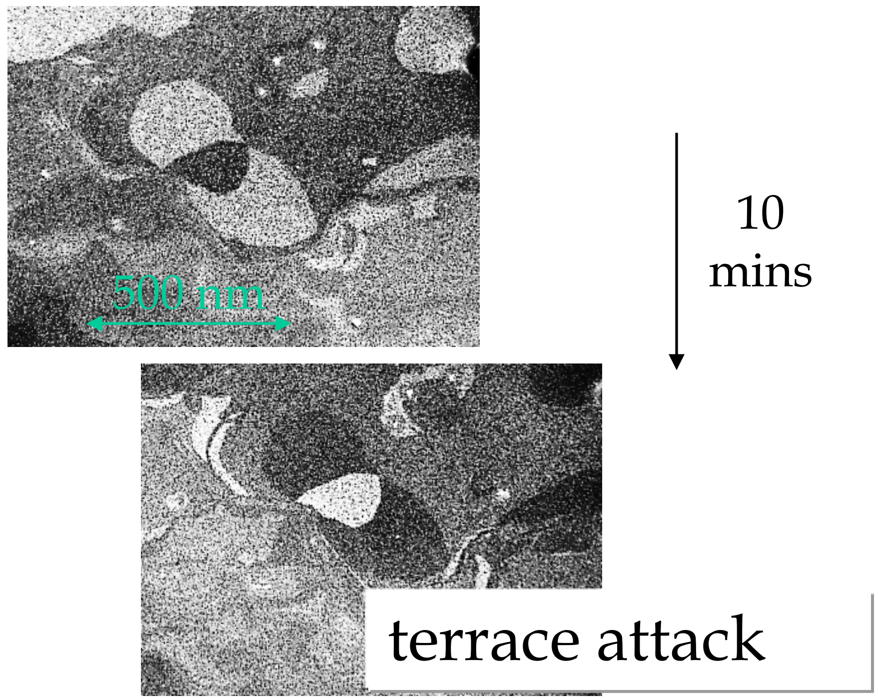

Ross, Gibson and Twesten, Surf. Sci. **310**, 243 (1994)

Diffuse scattering

VOLUME 81, NUMBER 18 PHYSICAL REVIEW LETTERS 2 NOVEMBER 1998

Paired and Unpaired Charge Stripes in the Ferromagnetic Phase of $La_{0.5}Ca_{0.5}MnO_3$

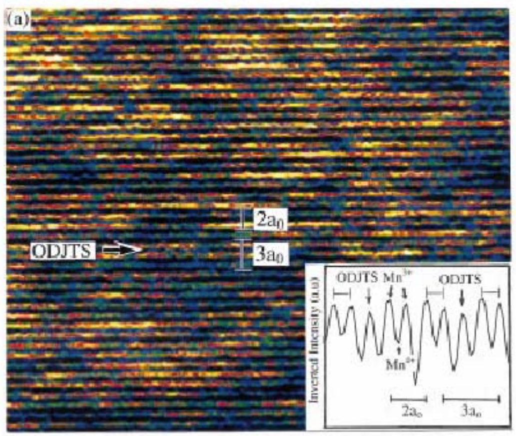

S. Mori,[1,*] C. H. Chen,[1] and S-W. Ch
Laboratories, Lucent Technologies, Murray Hil
Physics and Astronomy, Rutgers University, P
(Received 9 April 1998)

existence of ferromagnetism and charge order
nogenous spatial mixture of incommensurate
crodomains with a size of 20–30 nm. Furtheri
te charge-ordered microdomains indicate a char
d Jahn-Teller distorted Mn^{3+} stripes. We prop
g of the d_{z^2} orbitals. These results demonstra
separation. [S0031-9007(98)07522-X]

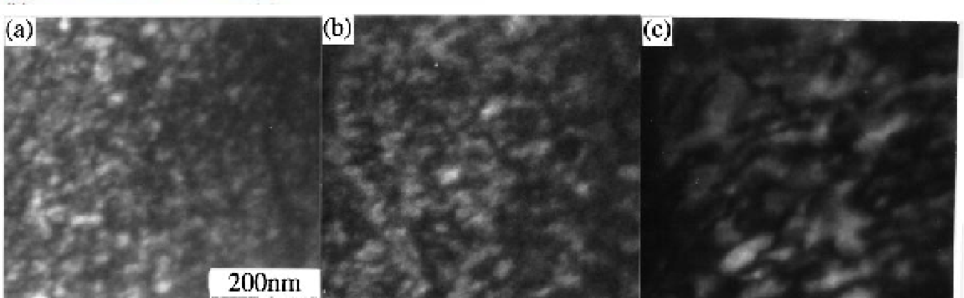

temp/ dep. domains (dark-field)

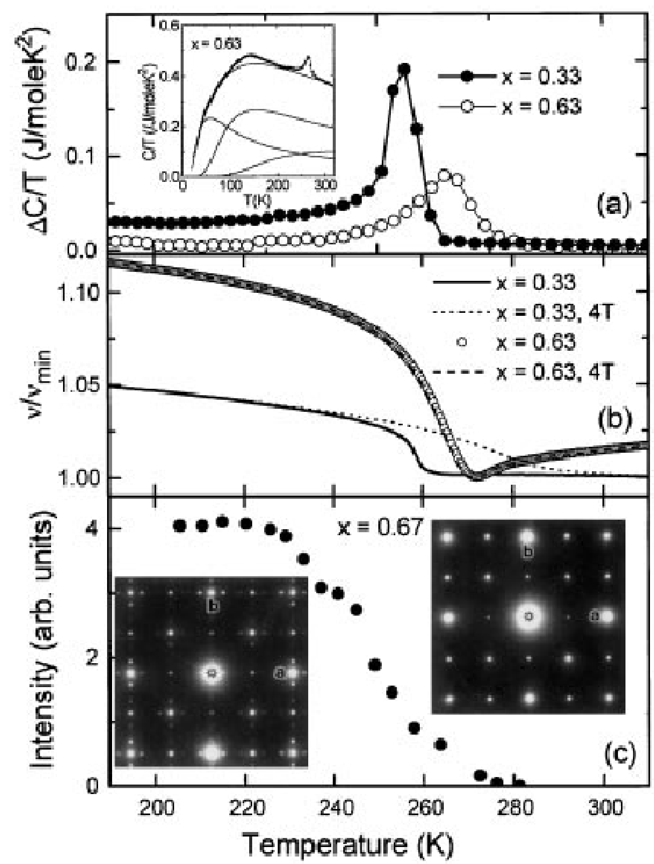

Structural Biology

Phasing reflections for large structures

Three-Dimensional Structure of a Recombinant Gap Junction Membrane Channel

Vinzenz M. Unger,[1]* Nalin M. Kumar,[1] Norton B. Gilula,[1]
Mark Yeager[1,2]†

Gap junction membrane channels mediate electrical and metabolic coupling between adjacent cells. The structure of a recombinant cardiac gap junction channel was determined by electron crystallography at resolutions of 7.5 angstroms in the membrane plane and 21 angstroms in the vertical direction. The dodecameric channel was formed by the end-to-end docking of two hexamers, each of which displayed 24 rods of density in the membrane interior, which is consistent with an α-helical conformation for the four transmembrane domains of each connexin subunit. The transmembrane α-helical rods contrasted with the double-layered appearance of the extracellular domains. Although not indicative for a particular type of secondary structure, the protein density that formed the extracellular vestibule provided a tight seal to exclude the exchange of substances with the extracellular milieu.

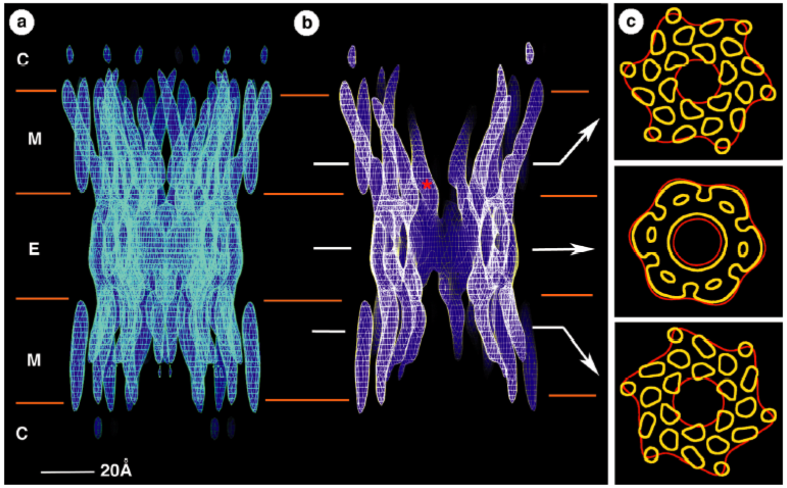

SCIENCE VOL 283 19 FEBRUARY 1999 1177

A ratchet-like inter-subunit reorganization of the ribosome during translocation

Joachim Frank*†‡ & Rajendra Kumar Agrawal†‡

* *Howard Hughes Medical Institute, † Health Research Incorporated at the Wadsworth Center, and ‡ Department of Biomedical Sciences, State University of New York at Albany, Empire State Plaza, PO Box 509, Albany, New York 12201-0509, USA*

The ribosome is a macromolecular assembly that is responsible for protein biosynthesis following genetic instructions in all organisms. It is composed of two unequal subunits: the smaller subunit binds messenger RNA and the anticodon end of transfer RNAs, and helps to decode the mRNA; and the larger subunit interacts with the amino-acid-carrying end of tRNAs and catalyses the formation of the peptide bonds. After peptide-bond formation, elongation factor G (EF-G) binds to the ribosome, triggering the translocation of peptidyl-tRNA from its aminoacyl site to the peptidyl site, and movement of mRNA by one codon[1]. Here we analyse three-dimensional cryo-electron microscopy maps of the *Escherichia coli* 70S ribosome in various functional states, and show that both EF-G binding and subsequent GTP

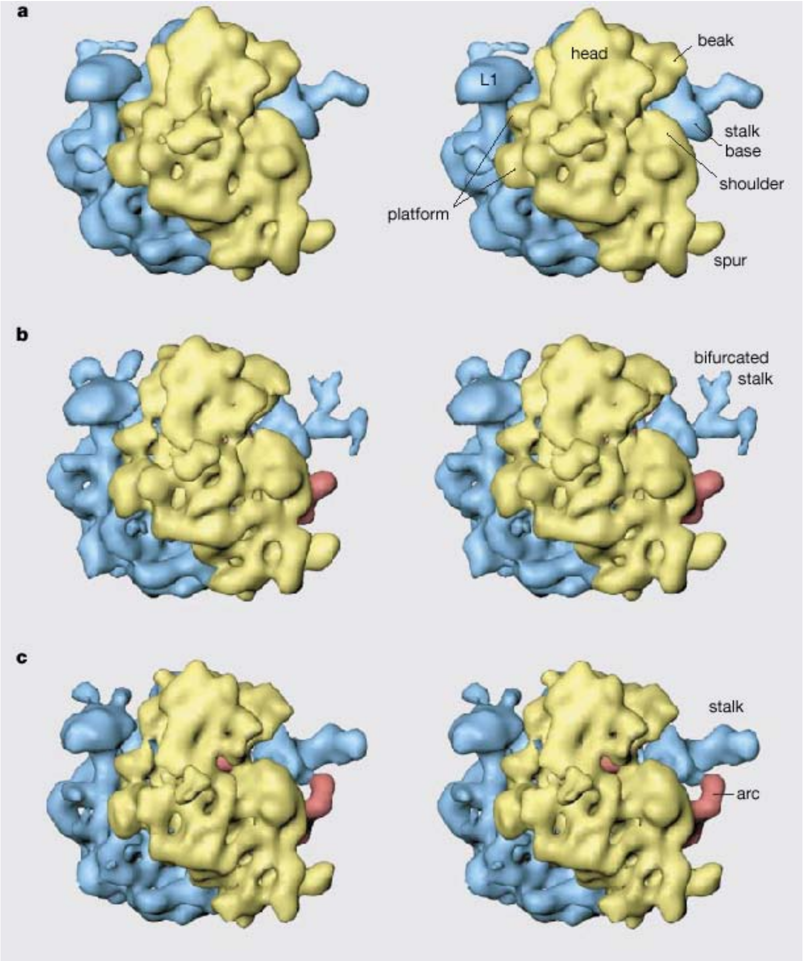

x-ray structure this year depended on 7.5 Å e-structure

Nanoscience

VOLUME 85, NUMBER 3 PHYSICAL REVIEW LETTERS 17 JULY 2000

Nanomechanics of Individual Carbon Nanotubes from Pyrolytically Grown Arrays

Ruiping Gao,[1,4] Zhong L. Wang,[1,*] Zhigang Bai,[1] Walter A. de Heer,[2] Liming Dai,[3] and Mei Gao[3]
[1]*School of Materials Science and Engineering, Georgia Institute of Technology, Atlanta, Georgia 30332-0245*

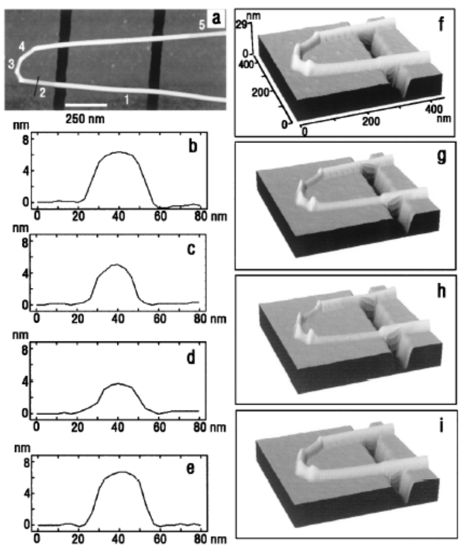

FIG. 1. Deformability of a MWCNT deposited on a patterned silicon wafer as visualized with tapping-mode AFM operated far below mechanical resonance of a cantilever at different set points. The height in this and all subsequent images was coded in gray scale, with darker tones corresponding to lower features.

AFM - *Yu et. al.*
*PRL **85**, 1456, (2000)*

shear modulus

$$\nu_i = \frac{\beta_i^2}{8\pi} \frac{1}{L^2} \sqrt{\frac{(D^2 + D_1^2)E_b}{\rho}},$$

E~30 GPa
without defects

E~3 GPa
with defects

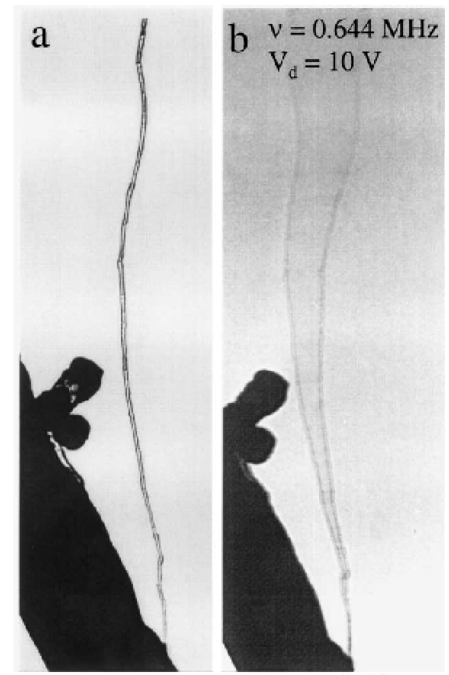

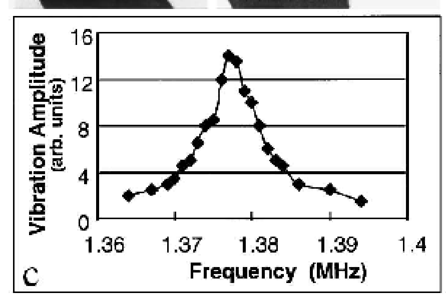

VOLUME 81, NUMBER 9 PHYSICAL REVIEW LETTERS 31 AUGUST 1998

Size Effects in Carbon Nanotubes

C.-H. Kiang,[1] M. Endo,[2] P. M. Ajayan,[3] G. Dresselhaus,[4] and M. S. Dresselhaus[5]

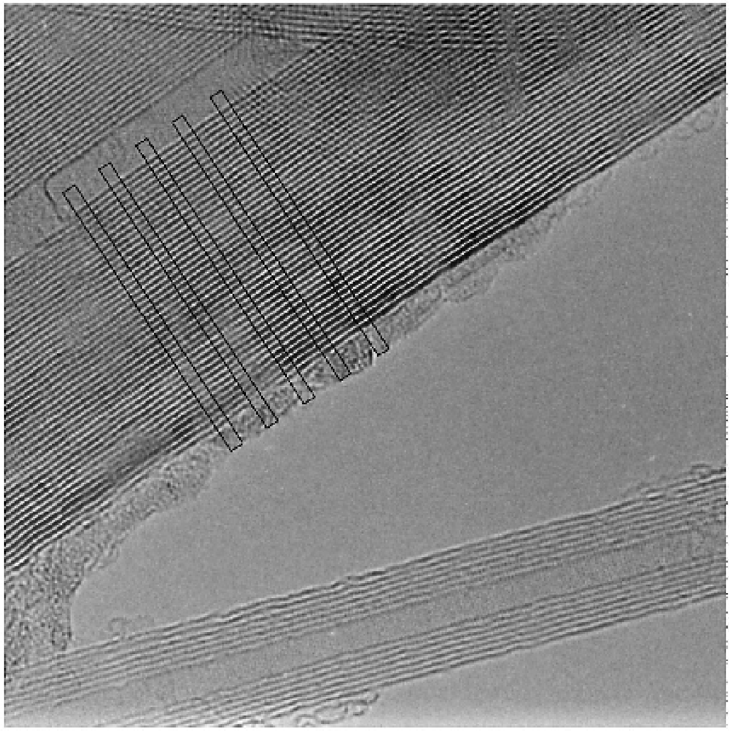

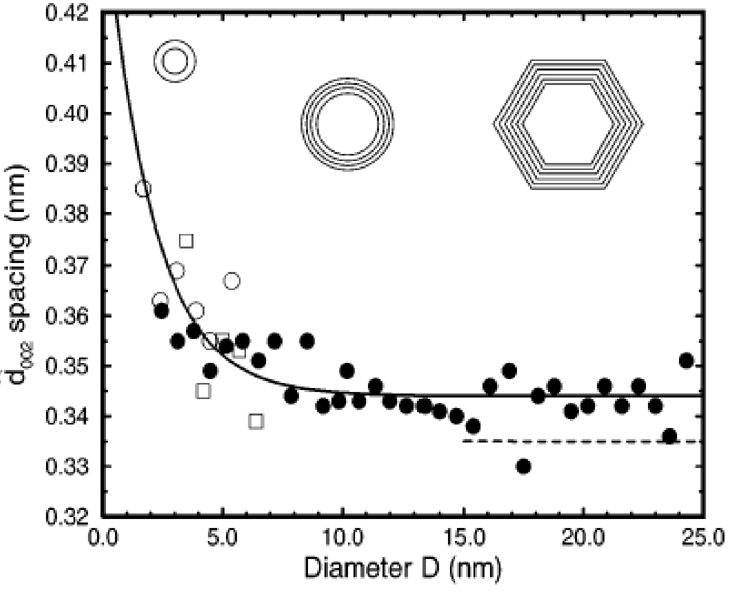

helicity plays a role in properties/structure

Applications of Z Contrast

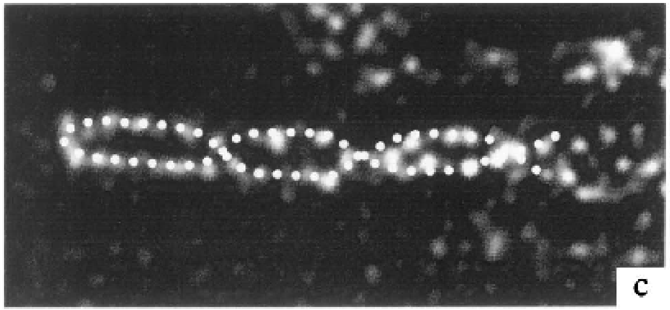

Iodine atoms in 1nm diameter C-SWNT
*Fan. et al. PRL **84**, 4621 (2000)*

Hard X-ray Nanoprobe

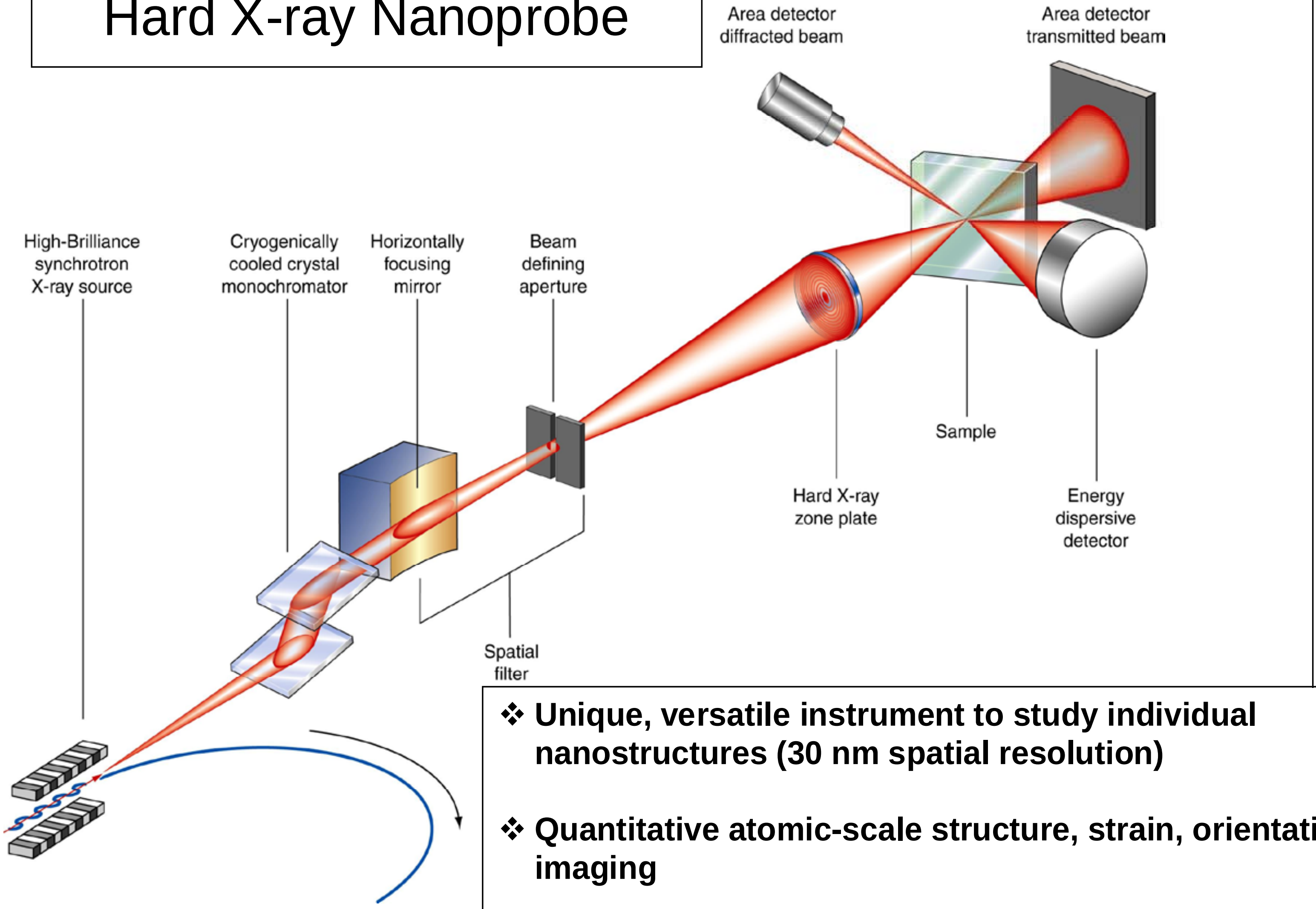

- ❖ **Unique, versatile instrument to study individual nanostructures (30 nm spatial resolution)**
- ❖ **Quantitative atomic-scale structure, strain, orientation imaging**
- ❖ **Sensitive trace element and chemical state analysis**
- ❖ **Ability to penetrate overlayers, environments, fields**

Zone Plate

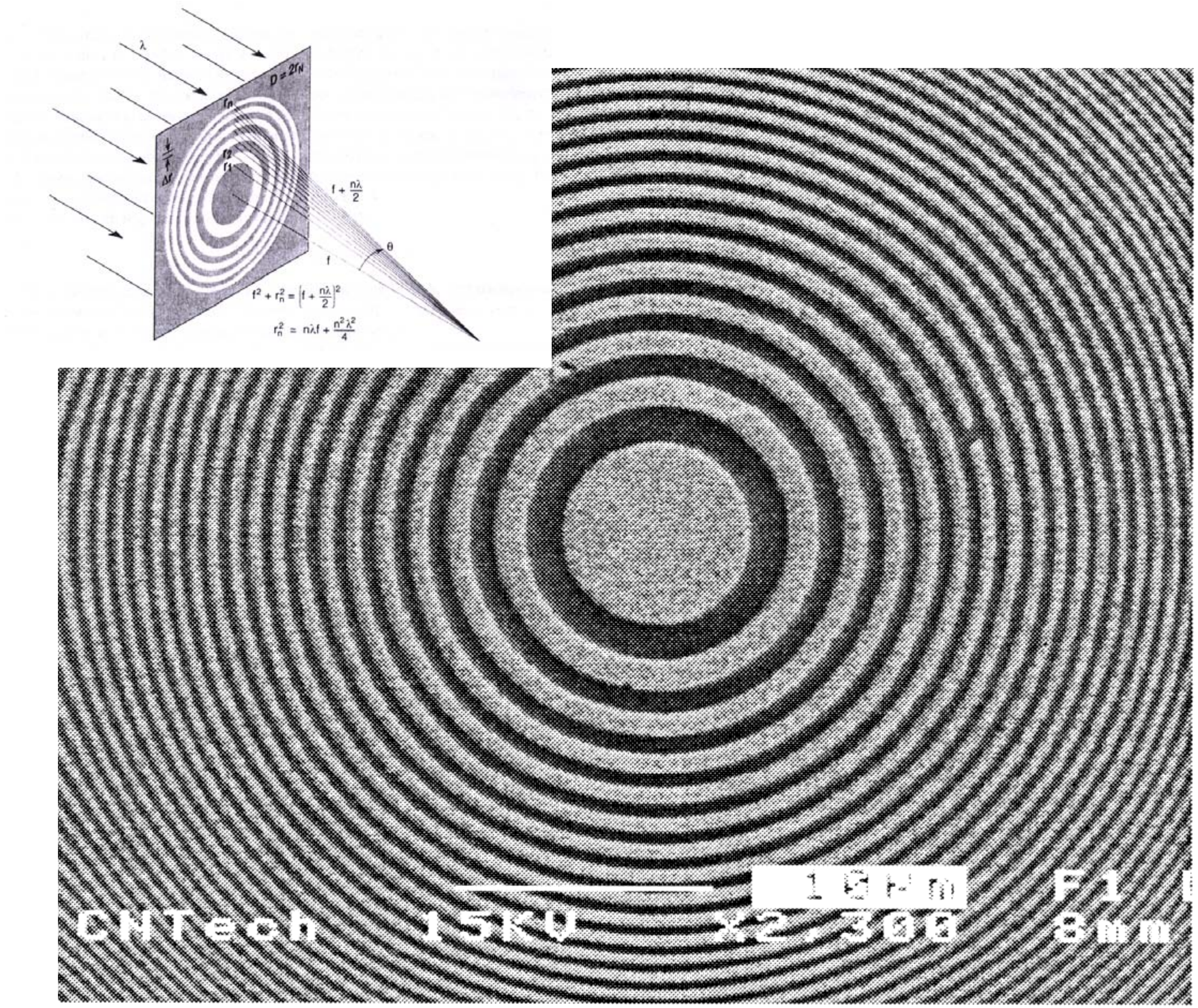
λ
D = 2r_N
r_n
r_2
r_1
Δr
f + nλ/2
θ
f
f² + r_n² = (f + nλ/2)²
r_n² = nλf + n²λ²/4
10μm
CHTech 15KV X2,300 8mm

X-ray Microprobe Experiments

Nanometer-scale physics in ferroelectrics (P. Evans, Lucent)

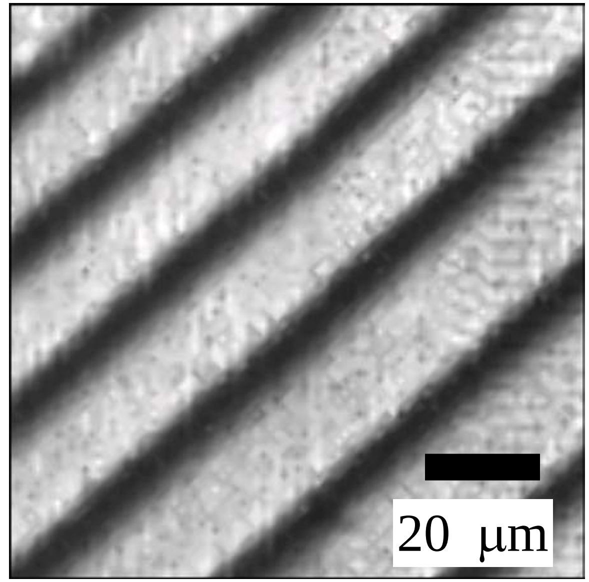

Magnetization in $HoFe_2$

J. Pollmann, *et al.*, Rev. Sci. Instrum. **71** 2386 (2000).

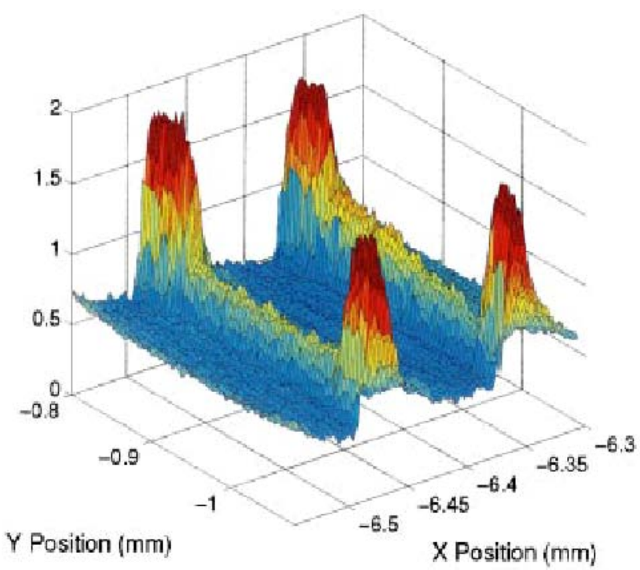

Stress under metallization on Si (100)

P.-C. Wang, *et al.*, Appl. Phys. Lett. **76** 3726 (2000).

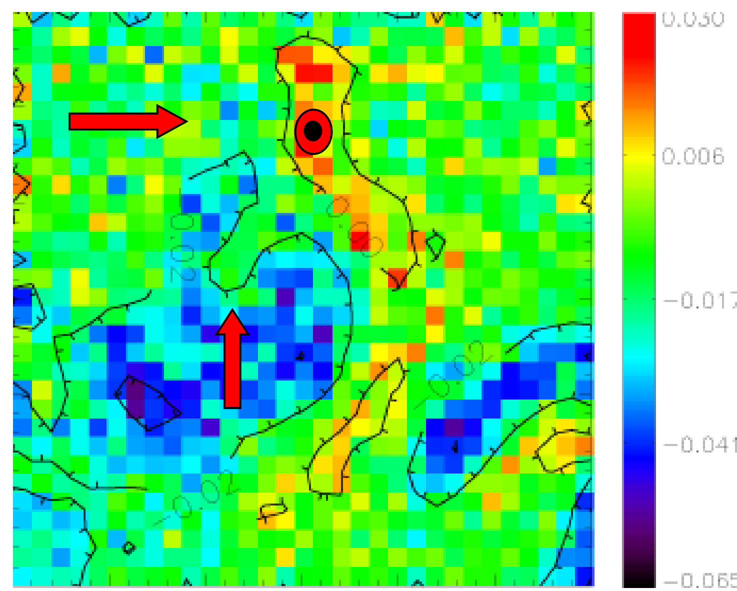

Real-Time X-ray Characterization of Patterned Growth

P. Fini *et al.*, *APL* **76,** 3893 (2000)

Growth morphology (ex-situ SEM):

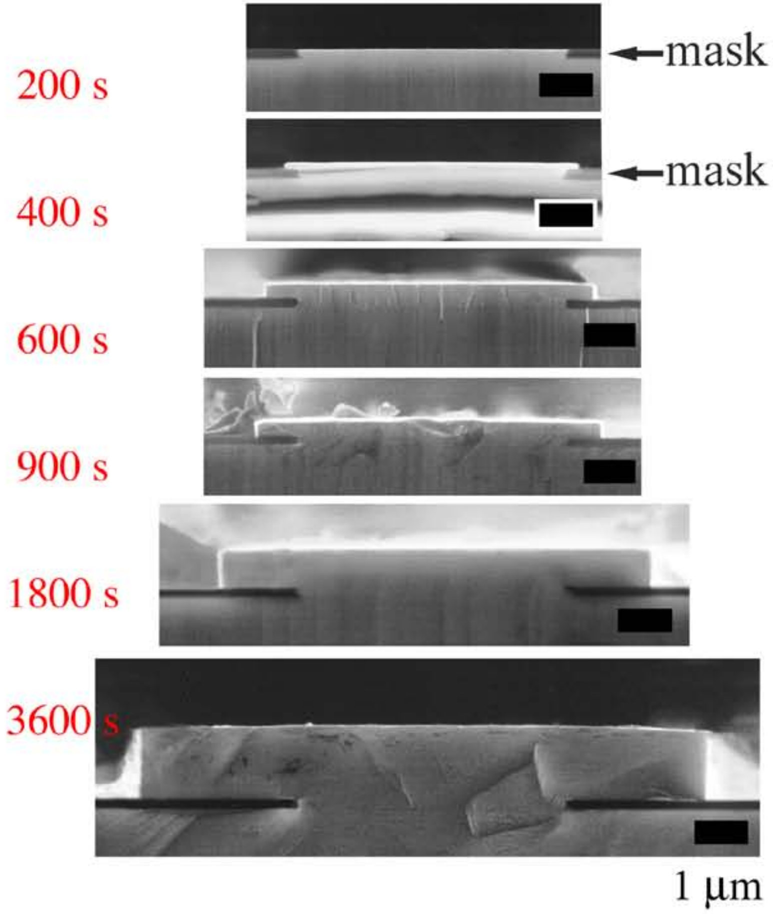

In-situ X-ray measurement of wing tilt during growth:

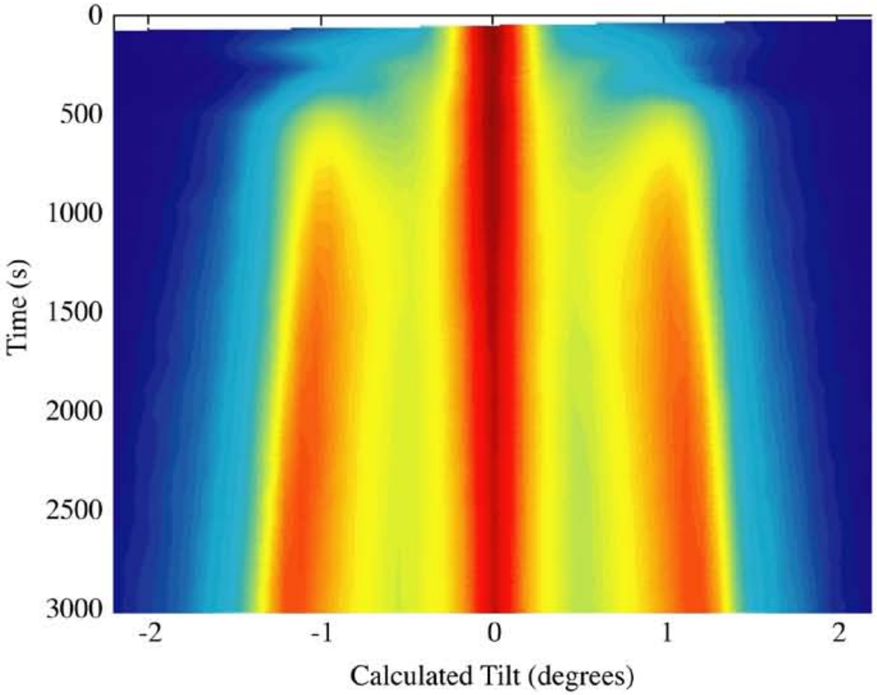

Wing tilt occurs at outset of overgrowth, not during cooling

Nanoprobe diffraction studies of Nanopatterning - ETCHING

- Microfocused beam will allow illumination of individual nanostructures.
- Need to understand subtractive processes as well as additive (growth)
- Novel materials will be investigated (e.g., multicomponent oxides).

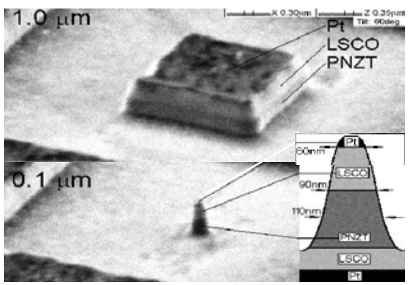

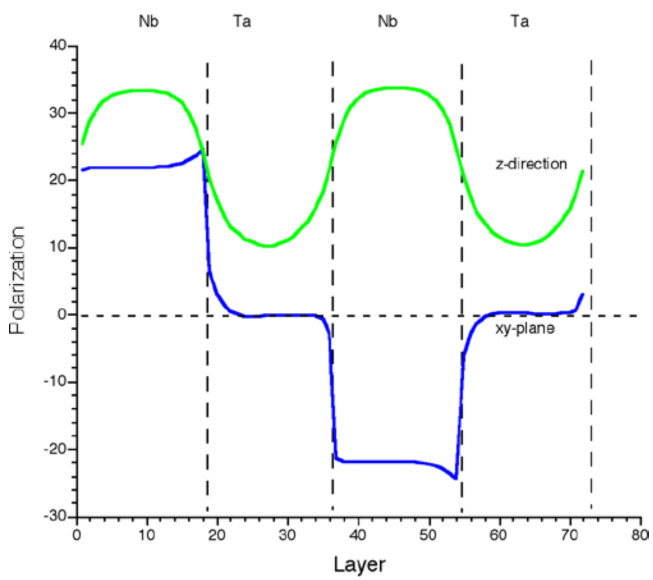

hybrid structures

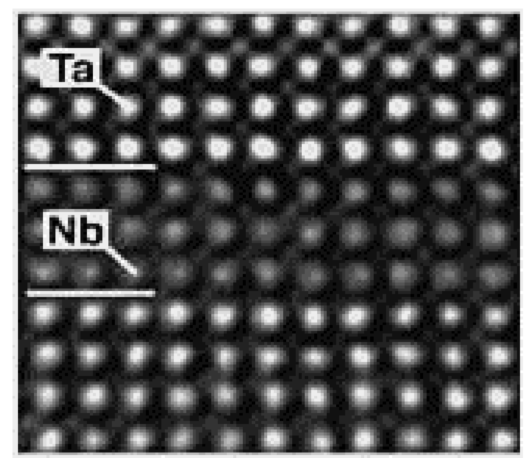

H. M. Christen et al., APL, 72 2535 (1998)

Studies of Growth and Etching

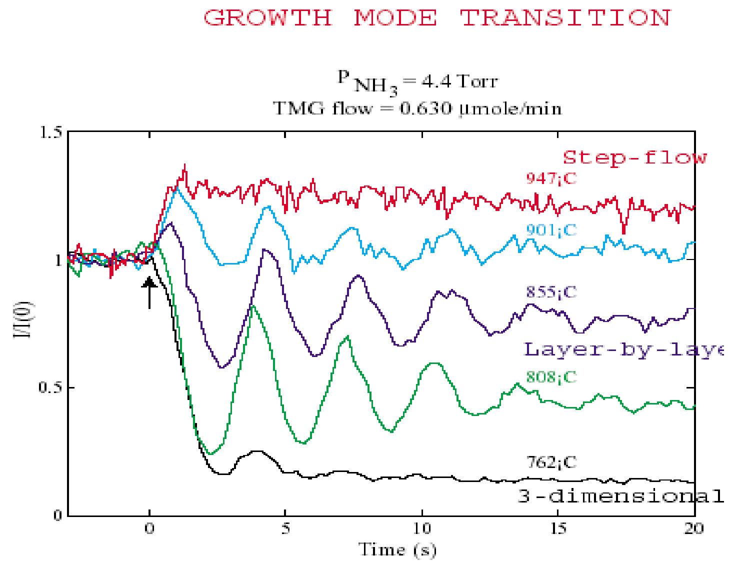

Oscillations in the crystal truncation rod intensity during MOCVD growth of GaN
APL **74**, 3326 (1999).

Time-Resolved Studies of Ferroelectric Switching

- Lattice parameter during switching has been measured with 17 nsec time resolution.
- Two-step response to voltage: prompt piezoresponse followed by switching on ~ 100 nsec time scale.

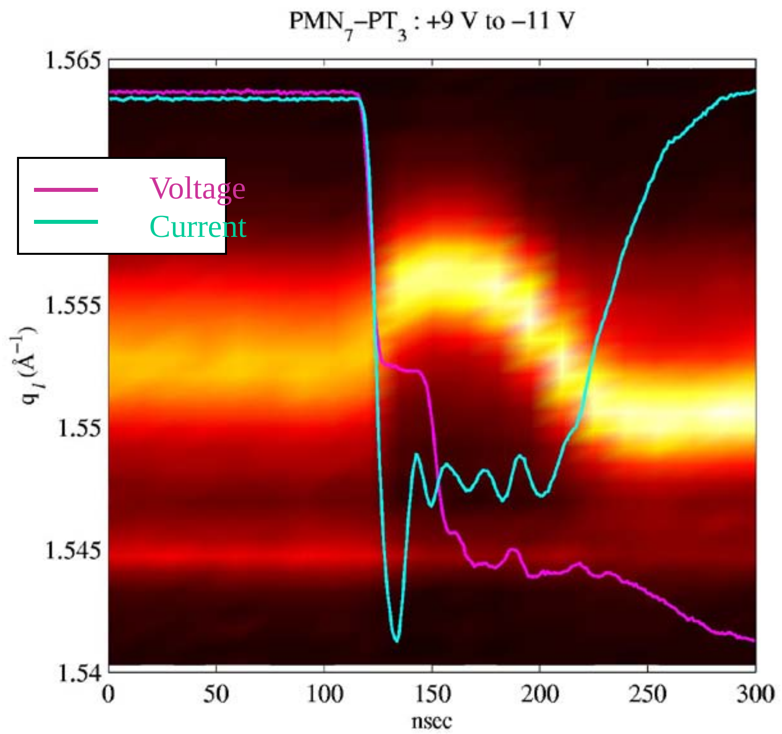

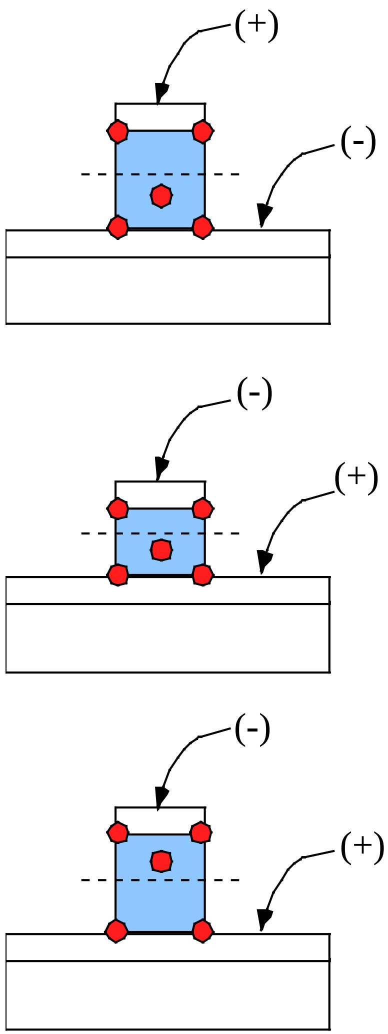

C. Thompson (NIU), S. Streiffer (ANL-MSD), A. McPherson (ANL-XFD)

Measurement of Strain in Al-Cu Interconnect Lines Using X-ray Microdiffraction

- Reliability of integrated circuit Al-Cu interconnects in electronics impacted by electromigration and mechanical stress.
- X-ray microdiffraction from interconnects reveals origin and details of microscopic stress.
- Can lead to increasingly reliable devices (computers, etc.) even as they become more complex.

H. Solak et al., J. Appl. Phys 86, 884 (1999).

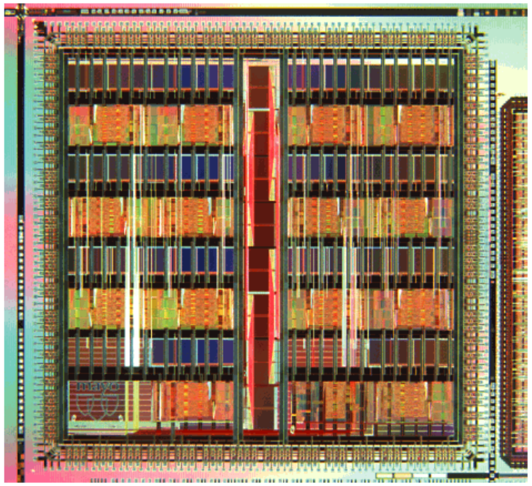

Fast Fourier transform integrated circuit (Special Purpose Processor Development Group, Mayo Clinic)

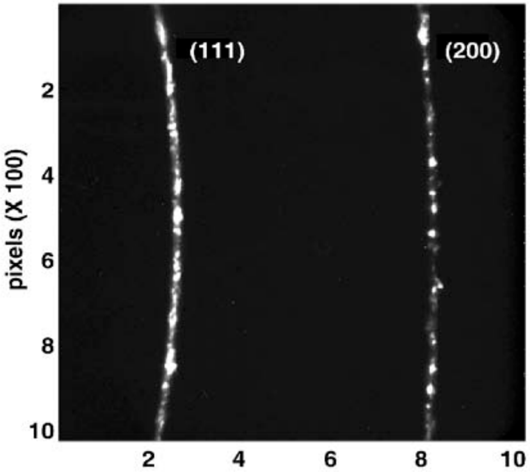

Microdiffraction pattern from a thick-blanket Al-Cu film.

X-Ray Fluorescence Microscopy - complementary to Transmission Electron Microscopy

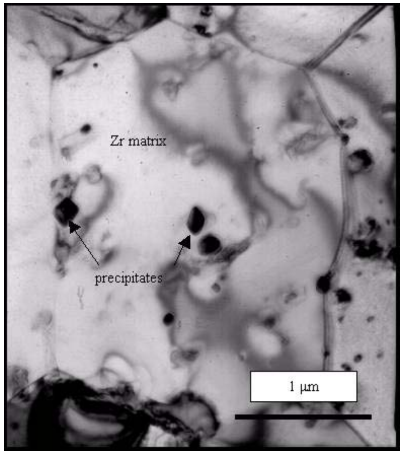

Transmission Electron Microscopy of Zircalloy grain

	Zircaloy-4 (weight %)	ZIRLO (weight %)
Fe	0.24	0.11
Cr	0.11	0.001
Sn	1.64	1.08
Ni	0.0034	<0.001
Nb	-	1.23
O	0.112	0.145
Cu	0.002	0.002
Hf	<0.004	<0.004

Measured overall compositions

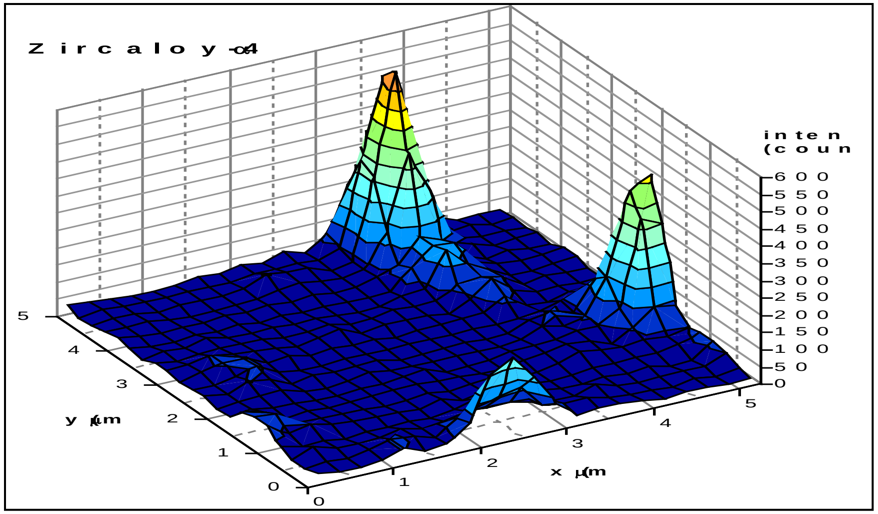

Examining compositions in metal alloy precipitates

X-Ray fluorescence imaging of single bacterial cells

Kemner et al. Science 306, 686 (2004).

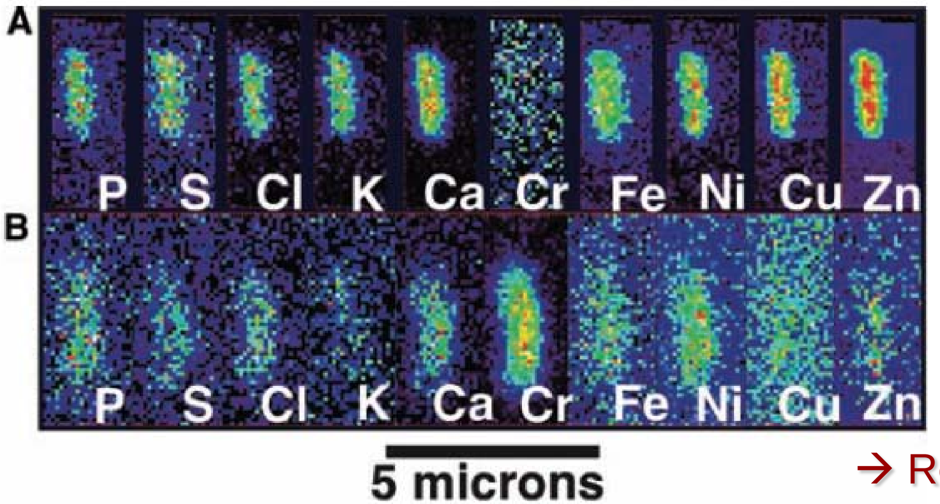

Fig. 1. False-color micro-XRF maps of qualitative spatial distributions and concentration gradients of elements in and around planktonic *P. fluorescens* microbes harvested before (A) and after (B) exposure to potassium dichromate [Cr(VI)] solution (1000 ppm) for 6 hours.

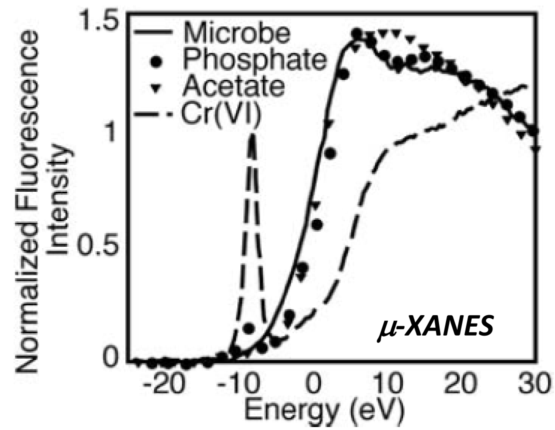

→ Redox states Cr(III)

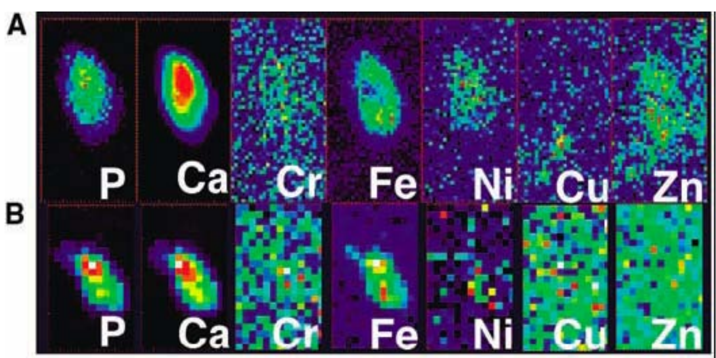

A: planktonic bacterium cell before exposure to Cr

B: planktonic cell after exposure to 1000 ppm Cr(VI)

Isolated planktonic cell accumulates Cr, looses 'typical' cellular elements, and stains 'dead'

Surface adhered cell does not take up Cr, shows no change in elemental content, and remains alive

Attachment of prokaryotic cells to surfaces modulates elemental content and response to environmental challenges

Advanced X-ray imaging reveals hierarchical structure

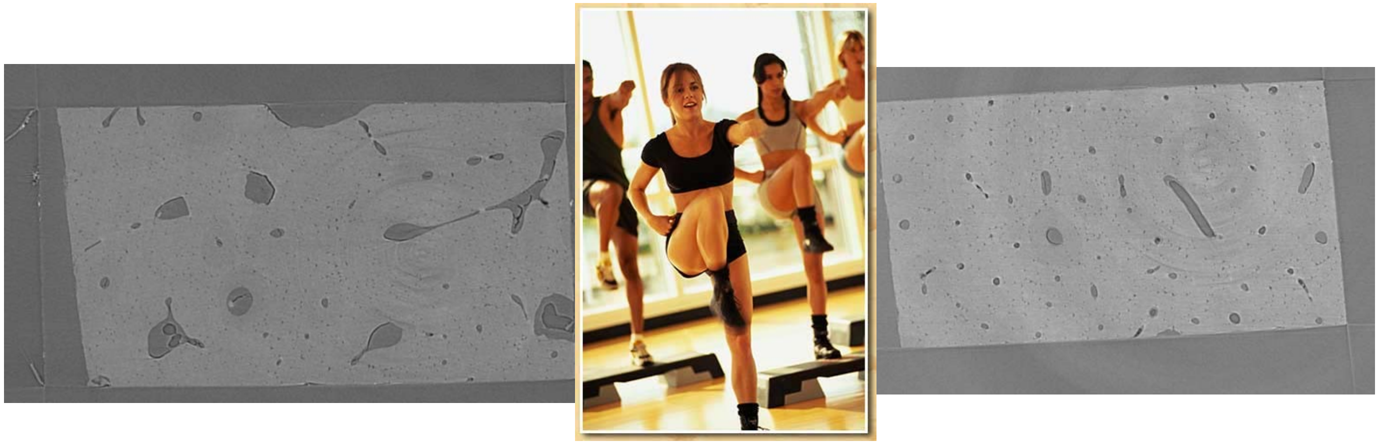

The effect of different exercise regimens on bone – S. Stock, NWU 2-BM

Big bugs, Socha et al., PNAS **104**, 13198, (2007)

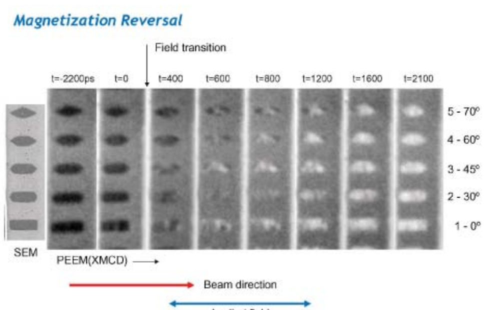

Magnetic instability regions in patterned structures
Han et al., Phys. Rev. Lett. **98**,
147202 (2007)

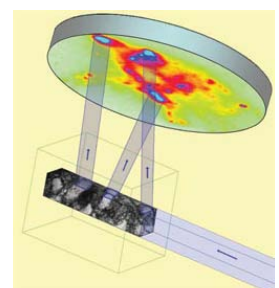

Dislocation walls are lumpy,
Levine et al., Nat. Mater. **5**, 619 (2006)

Coherent X-Ray Diffraction

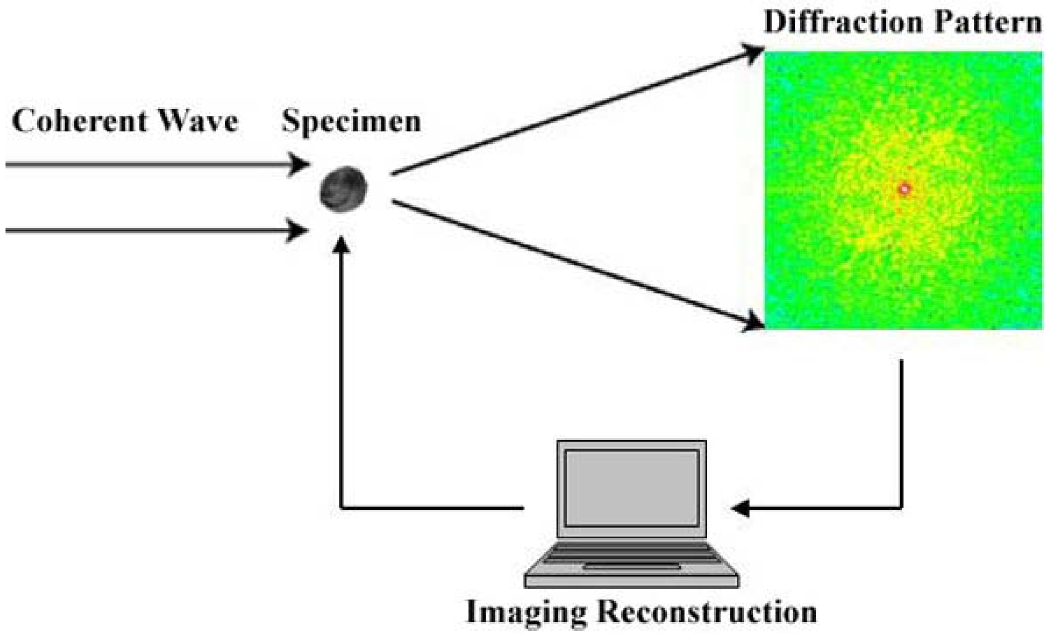

- ➔ Coherent diffraction imaging is much like crystallography but applied to noncrystalline materials
- ➔ First proposed by David Sayre in 1980, and first experimental demonstration by John Miao et al in 1999 using soft x-rays
- ➔ Requires a fully coherent x-ray beam

Analogous to crystallography

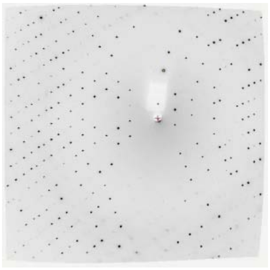

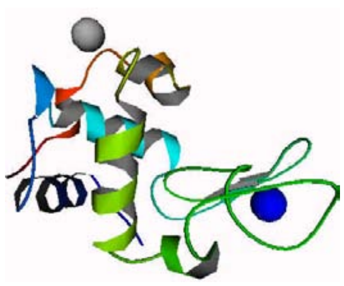

Miao et al. (1999)

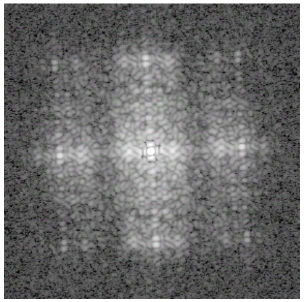

Soft x-ray speckle of static aerogels

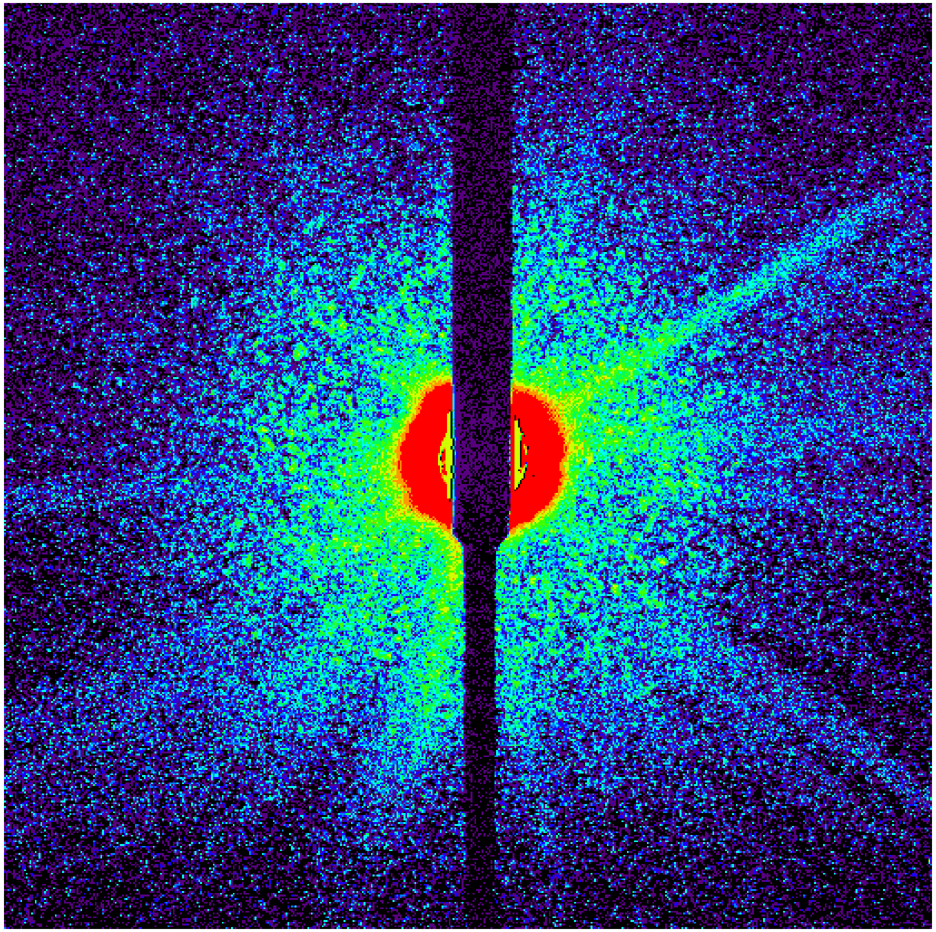

Speckle pattern produced by aerogel sample (0.014 g/cm^3). Pattern was recorded with 1.83 keV x-rays using a 5-µm pinhole source and monochromatic ($E/\Delta E \sim 1000$) beam.

Ian McNulty, APS

Surface dynamics of polymer films

- Motivated by reports that T_g at the surface of polymer films is reduced Kim, Ruehm, Lurio, Basu, Lal, Mochrie, and Sinha used XPCS at 8-ID to characterize the relaxation of thermally excited height fluctuations on the surface of polystyrene(PS) films to investigate how the near-surface viscosity might differ from that of the bulk PS.

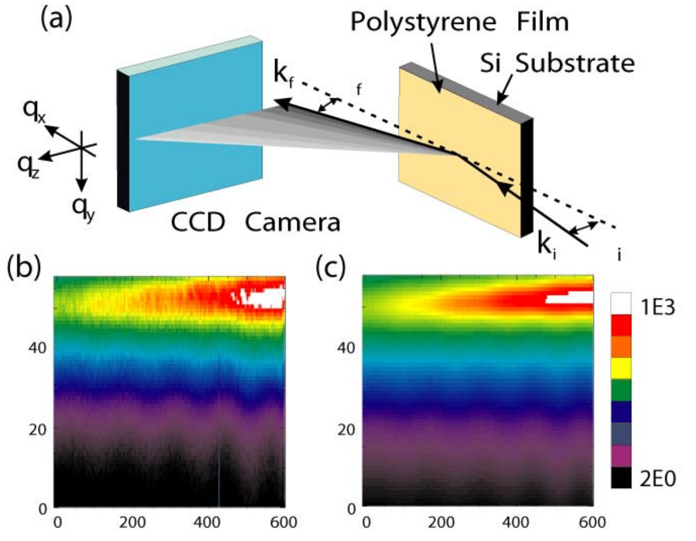

Surface Dynamics of Polymer Films

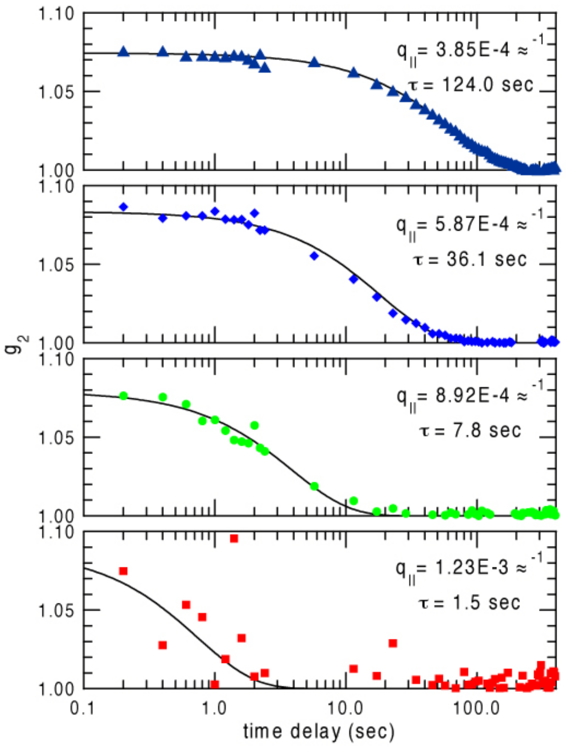

Intensity correlation of the reveals the characteristic relaxation times for capillary waves

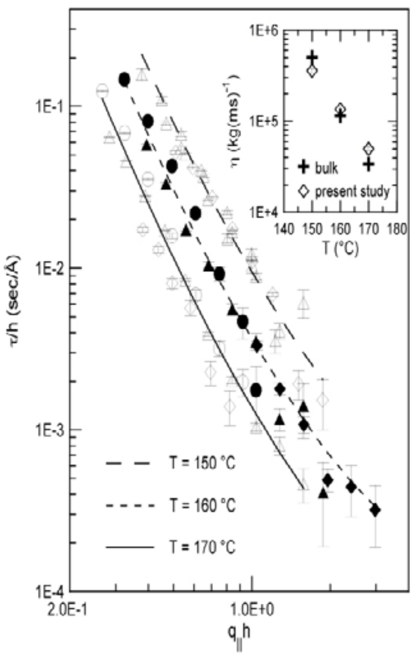

Shows no change in T_g near surface

Fluctuation (Electron) Microscopy

Diffraction

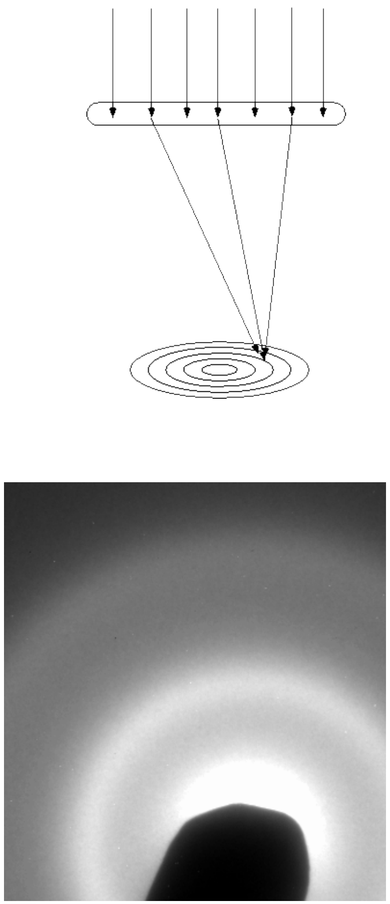

Microdiffraction
"Speckle Diffraction"

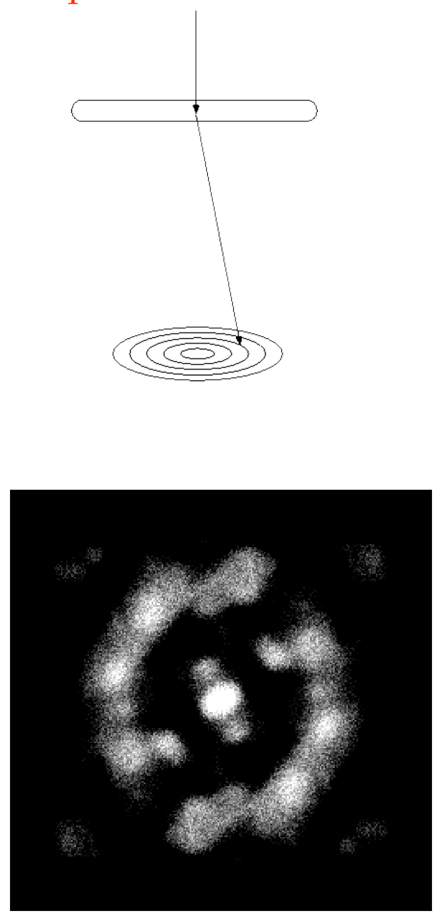

Speckle Imaging

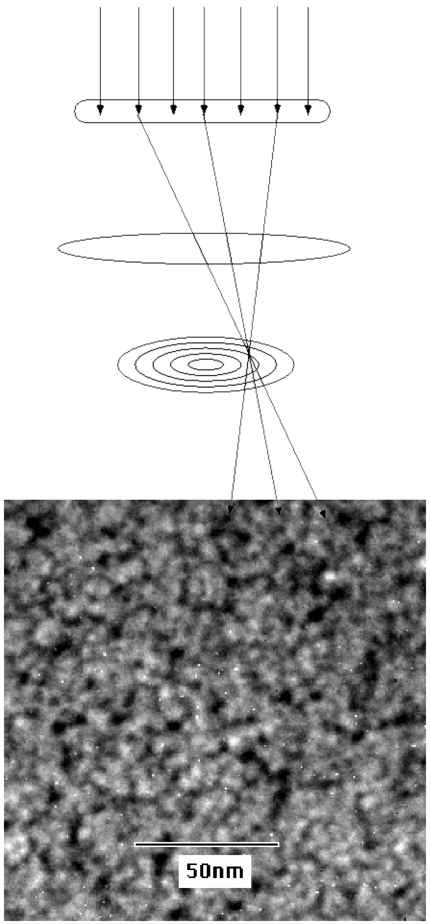

"coherent diffraction"

New structural information from glasses - Fluctuation Microscopy

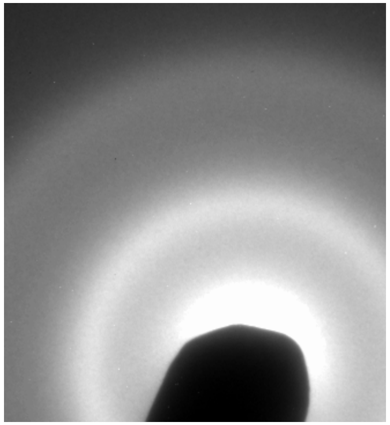

Diffraction => Pair Correlation Function

=>short-range order

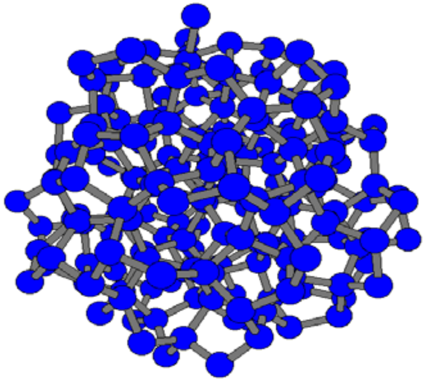

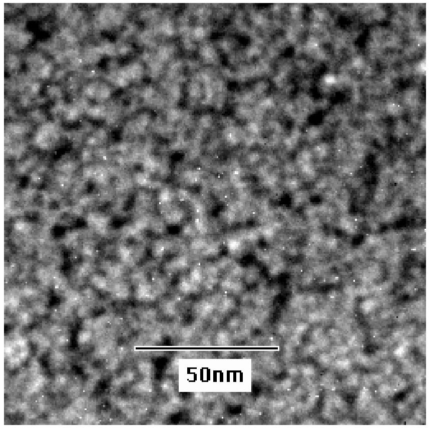

Imaging (speckle) =>Pair-Pair Correlation Function

=>medium-range order

Paracrystallinity in a-Si/Ge

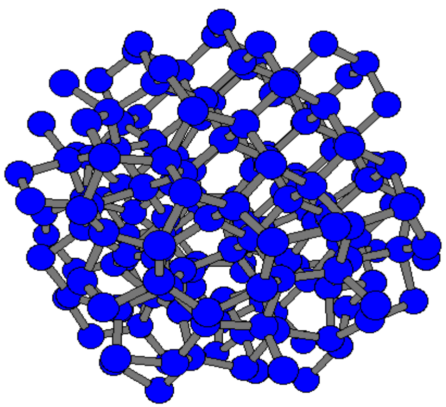

Medium-range order (~15Å) found in deposited amorphous semiconductors
 - not seen by diffraction

Important effects on thermodynamic and physical properties - electrical stability, impurity diffusion

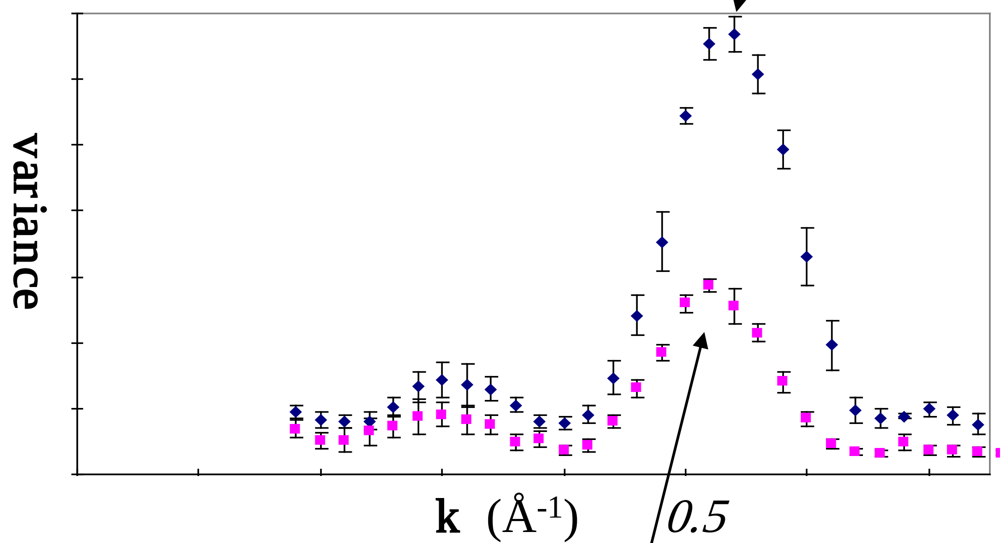

Become more like random networks on annealing *or light soaking in a-Si(H)*

Gibson et. al., Phys. Rev. Lett. **78**, 1074 (1997); Appl. Phys. Lett **73**, 3093 (1998).

Further Reading

- “**Electron Microscopy of Thin Crystals**”, Hirsch et. al. (Kreiger, New York 1977)
- “**Diffraction Physics**”, J.M. Cowley, (North Holland, Amsterdam 1981)
- “**Transmission Electron Microscopy**”, L. Reimer, (Springer-Verlag, Berlin 1984)
- “**Transmission Electron Microscopy: A Textbook for Materials Science**”, D.B. Williams and C.B. Carter, (Plenum, New York 1996)